Generation Reliability for Isolated Power Systems with Solar, Wind and Hydro Generation

Jimmy Ehnberg

Department of Electric Power Engineering
CHALMERS UNIVERSITY OF TECHNOLOGY
Göteborg, Sweden 2003

THESIS FOR THE DEGREE OF LICENTIATE OF ENGINEERING

Generation Reliability for Isolated Power Systems with Solar, Wind and Hydro Generation

Jimmy Ehnberg

Department of Electric Power Engineering
CHALMERS UNIVERSITY OF TECHNOLOGY
Göteborg, Sweden 2003

Generation Reliability for Isolated Power Systems with Solar, Wind and Hydro Generation

Jimmy Ehnberg

Technical Report No. 478L
ISSN: 1651-4998

Department of Electric Power Engineering
CHALMERS UNIVERSITY OF TECHNOLOGY
SE-412 96 Göteborg
Sweden
Telephone + 46 (0)31 772 1000

Chalmers Bibliotek, Reproservice
Göteborg, Sweden 2003

Abstract

This licentiate thesis deals with reliability issues for small isolated power systems. The focus is on power systems in remote areas based entirely on renewable energy sources. The sources investigated in this thesis are mainly solar and wind power and models for these energy sources are presented.

The solar power model is based on the solar declination and cloud coverage. In addition a Markov theory based model for simulating cloud coverage data is presented. The wind power model is based on two Markov chains, one for low wind and one for high wind. Both the solar and the wind models use measurements as input but by using normalised wind speed measurements a more general wind speed model is obtained. There are still, but minor, needs for site-specific meteorological measurements.

The presented models of solar and wind power are together with some simpler models of hydro power, storage and loads used for case studies. Since the solar model is dependent on the location, a site in Africa is used. Timbuktu in Mali was chosen for its subsahara climate and the fact that Mali is considered a developing country. Twelve cases were studied with combinations of solar, wind and hydro power both with and without storage possibilities.

A case study with only wind as power source has a higher overall availability then one with only solar power. But since all the solar power is available during daytime the availability is higher for solar power during daytime. By adding storage capability the overall availability will be higher for solar power because more efficient use of the storage. Combining the power sources with small hydro power (only 10% of total maximum load) the availability will be significantly increased. The hydro power will then supply the load during low load hours.

A combination of all three power sources gives a high reliability because during the high daytime load all three sources are available and during nighttime both wind and hydro are available. The largest availability problems are during mornings and evenings when the load is high but the solar power has a low availability. This effect is season dependent.

To be able to use exclusively renewable energy sources a combination of sources is needed to secure the reliability of the supply.

Keywords: Renewable energy, Stochastic modelling, Generation reliability, Isolated power systems, Solar power, Wind power.

Acknowledgement

First, I would like to thank Professor Math Bollen for initiating the project with AGS and for the support and encouragement. His support was always there and the "door was always open" in case of problems and short questions.

I will also thank Professor Stanislaw Gubanski and Assistant Professor Jörgen Blennow for teaching me the basics of being a Ph.D student and Yuriy Serdyuk, room-mate, for sharing his experience in the field of academic work with me.

I would like to thank the Alliance of Global Sustainability (AGS) for their financial support and Swedish Meteorological and Hydrological Institute (SMHI) and Hans Bergström at Uppsala University for providing meteorological data.

The colleagues at the department, for the help in different areas and making the department a fun place to work, should also be acknowledged. Also other friends, outside the department, for their support in their own way.

Finally, I will acknowledge Susanna and my parents for their understanding, encouragement and love throughout the project.

List of Publications

J.S.G. Ehnberg, M.H.J. Bollen, *"Simulation of global solar radiation based on cloud observations,"* International Solar Energy Conference, Gothenburg, May 2003.

J.S.G. Ehnberg, M.H.J. Bollen, *"Reliability of a small power system using solar power and hydro,"* Submitted to Electric Power Systems Research.

J.S.G. Ehnberg, M.H.J. Bollen, *"Reliability of a small isolated power system in remote areas based on wind power,"* Submitted to Nordic Wind Power Conference, Gothenburg, March 2004.

Contents

Chapter 1

Introduction

1.1 Isolated power systems

The use of electric power has increased during the last centuries and almost anyone needs electricity. Despite the wide coverage of large power systems, all costumers are not connected to a large power system. A small power system that is not connected to a much larger grid is called an isolated power system.

Example of isolated power systems are

- Cars
- Planes
- Ships
- Oil platforms
- Small islands
- Isolated villages far from a well-developed transmission and distribution grid.

How to provide power for the different small isolated power system varies due to surrounding conditions. The traditional source of energy in remote areas is wood but there are a shift to electric energy through diesel generators. The next, more environmentally-friendly, stage is introducing renewable sources like solar, wind and hydro power. One problem with use of diesel generators are transportation of the fuel. This is a major environmental hazard and high cost for a remote location.

A better solution is to use renewable energy sources: like solar, wind and hydro power. There are advantages and disadvantages of using renewables. The main advantages are that the system is environmental-friendly and there are very limited transport costs. A disadvantage is the uncertainty in power supply, which gives a lower reliability of the system.

Renewables are in most cases used as a complement to a diesel generator or to a large grid. The challenge however is to build a system with only renewables.

1.2 Stochastic modelling of renewables

Stochastic modelling of power sources is often done by assuming a constant generation capacity (often maximal) with planned interruptions and stochastic distribution of unplanned interruptions [1]. This model is valid for generators in power stations like nuclear and with fossil fuel. The method may even be applied to large scale hydro installation, albeit with some restrictions. For power stations that are dependent on the meteorological conditions this method is not applicable. Meteorologically dependent sources are e.g. solar and wind power.

The stochastic behavior of solar and wind power has a strong correlation with the weather. The amount of sunshine and the wind speed are not the only factors that affect the performance of the sources. Important other factors for solar power are temperature and shading [2], while for wind they are terrain, shading from other wind turbines and air density [3]. The shading from other wind turbines only affects the energy production in wind farms [4].

1.3 Aim of this study

The aim of this study is to gain understanding of renewable energy sources and interactions between sources. This will be done through development of stochastic models for renewable energy that can be used in power system reliability studies. The emphasis will be on the development of consistent models. The aim of case studies will be to prove the applicability of the models in the power system reliability studies.

Another issue is the need for meteorological data. We want models that can be applied to remote villages e.g. in the Mali desert or in the mountains of Tibet, without the need to do several years of measurements.

Other aims of this study are to indicate where more knowledge is needed and to function as a preparation for future projects with a multi-disciplinary approach.

This study is a part of a larger study within the Alliance for Global Sustainability (AGS). The larger study is a cooperation between Chalmers (Göteborg), ETH (Zürich), MIT (Boston), University of Tokyo and Shanghai Jiao Tong University. The main aim is to study isolated rural distribution networks with a large penetration of renewable sources. The study includes not only reliability issues but also source-system interfaces, social acceptance, controls and stability aspects and studies of currently used facilities in China and Africa. Each university is responsible for a part of the project.

1.4 Contents of this study

In this section each chapter is introduced and reading instructions are given according to the author.

Chapter 2: Generation Reliability

In this chapter the subject "generation reliability" is introduced. The most common techniques are discussed. Theories behind other methods used in the thesis are briefly introduced, such as Markov theory and Monte-Carlo simulation.

Chapter 3: Power System Models

This chapter presents the models used in this thesis.

A stochastic model of solar power based on cloud coverage observations and a method for simulating cloud coverage based on Markov theory are proposed. The section about solar power also contains a short presentation of some conversion technologies for solar power.

A model of hydro power is presented based on constant flow-of-river and a small reservoir.

A stochastic model of wind power is presented based on two Markov chains for simulating low and high wind. The mean value can be adapted to the one that exists at the investigated geographical location. The section about wind power also contains a short presentation of the most common conversion technologies for wind power.

A model for the load is also presented. The load model is based on both industrial and residential loads.

The chapter ends with some discussion regarding storage, both existing methods and future technologies and the model used in the case studies.

Chapter 4: Case Study, Timbuktu

In this chapter a case study is presented. Case study of Timbuktu in Africa is done with solar and wind power and combinations with and without hydro power and storage. The chapter ends with a comparison between different configurations of power sources.

Chapter 5: Conclusions

In this chapter the conclusions of this project are presented.

Chapter 6: Future Works

In this chapter some future research issues are identified.

Reading instructions

The main chapter is the case study and the model chapter contains the models used in the case study. Chapter two explains some techniques and conceptions used in the model chapter and in the case study. The reader may want to start by reading the case studies and use the other chapters as a resource base for further understanding of the models used.

Chapter 2

Generation Reliability

2.1 Hierarchical levels

Since a modern power system is complex, highly integrated and very large, even advanced computers will have problem to handle all in one entry. Therefore reliability studies of power systems are typically split into three so-called "hierarchical levels": generation, transmission and distribution [1].

The generation reliability (HLI) is the ability of the generation capacity to supply the load of the system, while the second hierarchical level (HLII) is transmission system and its ability to deliver the bulk supply. The third and lowest level (HLIII) is the complete system and its ability to supply individual consumers [1].

2.2 Level I reliability

The balance between load and generation is very basic in the operation of electric power systems. The balance is shown in a systematic way in Figure 2.1. At any moment in time generation and load should be equal, in accordance with the physical law of conservation of energy. This balance is the basis of the power-frequency control in interconnected power systems. Also for reliability assessment do we use this balance between generation and load but in a slightly different way. The load is compared with the so-called "generation capacity". The generation capacity is the sum of the power that can be produces by all generator units that are available to produce electrical energy. These units do not have to be operational but they should have the potential to be operational.

Generator units may be unavailable due to failures, this is called "forced unavailability", or due to preventive maintenance, this is called "planned unavailability". Both types of unavailability may be treated stochastically, but the planned unavailability is often treated deterministically. The uncertainty in the generation capacity is then only due to failures (outages) of generator units.

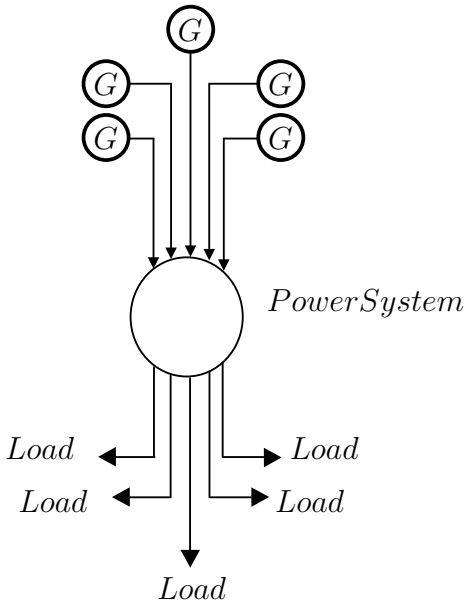

Figure 2.1: Model for generation reliability calculations.

2.3 Reliability quantifiers

In reliability calculations some quantifiers are normally used. Some of them are presented here according to the hierarchical level for which they are normally used [1].

Generation

LOLP (Loss Of Load Probability) = risk/probability that the load exceeds the generation capacity for a certain mix of generation and a certain load. Basic calculation is comparing the total generation (with its uncertainties due to failures/outages) with the annual peak load. This gives the probability that the maximum load cannot be supplied. Scheduled outages are typically not considered as maintenance is traditionally scheduled away from the annual peak.

LOLE (Loss Of Load Expectancy) = how much load that is lost, calculated over a number of short time intervals. For example daily peak loads over one year, or hourly loads during one year. Planned unavailability has to be considered in such a study.

Transmission

ELL (Expected load losses) = is the load that is expected to be lost. The value of ELL is often expressed in MW.

For HLII studies are also often LOLE used.

Distribution

SAIFI (System average interruption frequency index) = is the average interruption frequency per costumer. It is calculated as the ratio between total number of costumer interruptions and the total number of costumers.

SAIDI (System average interruption duration index) = is the average duration of an interruption per costumer. It is calculated as the ratio between the total time of costumers interruption duration and the total number of costumers.

ASAI (Average service availability index) and ASUI Average service unavailability index) = are the average time when the system is in service. They are calculated as the ration between costumers hours of availability/unavailability and hours of demand.

AENS (Average energy not supplied index)= is the average amount of energy that are not supplied and ACCI (average customer curtailment index) = are per costumer.

ENS (Energy not supplied index) = Is the power thatis missing supplied the load.

This thesis

In this thesis the terms availability and unavailability are used. Availability can be seen as the probability that the load will be supplied at an arbitrary chosen time. It is close to the LOLP but annual peak load is not considered. Unavailability is one minus the availability.

2.4 Reliability assessment

2.4.1 Generation capacity outage table

One of the most commonly used methods of determining the required generation for LOLE calculations is the generation capacity outage table [1]. If all units in a system were considered identical, but that is highly unlikely, an approach based on the binomial distribution could be used. The generation capacity outage table is based on the independent behavior of the different units were each has its own unavailability.

To illustrate this a simple numeric example is shown in Table 2.1. Consider a system with three units, two 4 MW and one smaller at 3 MW. The two 4 MW units have an availability of 0.97 while the 3 MW is more recently installed and has an availability of 0.98.

Table 2.1: The generation Capacity Outage Table for the considered system.

Capacity out of Service	Probability	Cumulative Probability
0	0.92208	1.00000
3	0.01882	0.07792
4	0.05704	0.05910
7	0.00116	0.00206
8	0.00088	0.00090
11	0.00002	0.00002
	1.00000	

The third column is the cumulative probability and that is the probability that more then that capacity is out of service. An example is that the probability that 4 MW or more is out of service is 0.05910.

This can easily be extended with more units to create a larger system by use of a recursive technique. In [1] this subject is discussed in more detail.

2.4.2 Frequency and duration method

The frequency and duration method is based on Markov theory but requires some more information regarding the system than the calculation of the Generation Capacity Outage Table [1]. The method also gives the average frequency and duration of interruptions as the title indicates.

The method needs input data like failure rate and repair time of the components. This method can easily be shown with a simple example with only two units, unit 1 with a failure rate of λ_1 and repair time of μ_1 and unit 2 with λ_2 and μ_2. There are four different states as shown in Table 2.2.

Table 2.2: Failure modes and states for the numerical example.

	State			
Unit	1	2	3	4
1	A	A	U	U
2	A	U	A	U

A=Generator is available.
U=Generator is unavailable.

The resulting state-space diagram is shown in Figure 2.2.

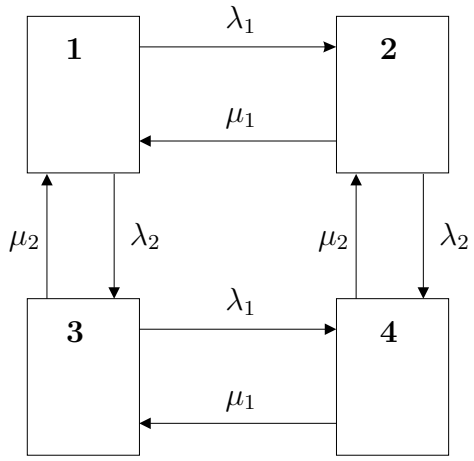

Figure 2.2: State-space diagram for the example.

By using this methods and theory of asymptotic solution of a Markov model frequency and duration may be calculated [5].

2.4.3 Markov models

The theory behind Markov chains and Markov processes is well know and are well explained in literature e.g. [5, 6, 7]. In this chapter is first the discrete Markov theory with finite states is introduced and then the continuous Markov theory with finite states. Markov theory is often used in reliability calculation not only in power systems but also in e.g. computer science or telecommunication (Theory of Queueing). Markov theory is also used for modelling stochastic behaviors like the models presented in this thesis.

In Equation 2.1 the Markov property is shown. The property is the fundamental equation in the Markov theory. A stochastic process that satisfies the Markov property is called a Markov process. The meaning of the Markov property is that the following value in the stochastic process is only dependent on the current value.

$$P(X_{n+1} = i_j | X_n = i_n, X_{n-1} = i_{n-1}, \ldots, X_0 = i_0) = P(X_{n+1} = i_j | X_n = i_n) \quad (2.1)$$

where X_n, n is an non-negative integer, is a discrete stochastic process with non-negative values and i_0 to i_n and i_j are values of that process.

Discrete Markov

In Equation 2.2 the definition of the transition probability is shown. The transition probability (p_{ij}) is the probability that the next value will be j if the current value is i.

$$P(X_{n+1} = j | X_n = i) = p_{ij} \quad (2.2)$$

The sum of the transition probabilities from a state is one, Equation 2.3 because there always has to come a next value that has to be something. The next value may be

the same value if the transition probability, p_{ii}, is non-zero. For an absorbing state the transition probability p_{ii} is one; it will never leave the state.

$$\sum_{j=1}^{k} p_{ij} = 1 \tag{2.3}$$

The transition probabilities can be summarized into a matrix (P), the so-called transition probability matrix. An example of a transition probability matrix can be seen in Equation 2.4.

$$P = \begin{pmatrix} p_{00} & p_{01} & p_{02} \\ p_{10} & p_{11} & p_{12} \\ p_{20} & p_{21} & p_{22} \end{pmatrix} \tag{2.4}$$

If the transition probability is dependent on time, see Equation 2.5, the process is called non-homogenous or non-stationary. In the models in this thesis only homogenous or stationary process are used and time or other dependencies are modelled through changes between homogenous processes.

$$P(X_{n+1} = j | X_n = i) = p_{ij}(n) \tag{2.5}$$

A Markov process is often shown graphically in the form of a state-space diagram. In the state-space diagram each state is represented by a node and all non-zero transition probabilities are marked as a transition between the nodes. A state-space diagram for a three state process is shown in Figure 2.3. The corresponding transition probability matrix is given in Equation 2.4. All the transition probabilities do not have to be non-zero.

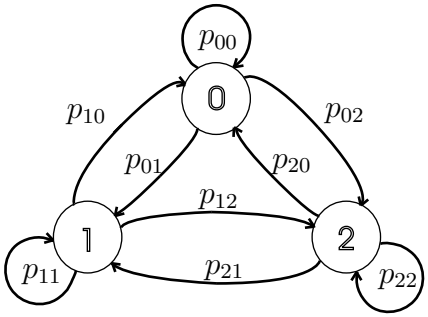

Figure 2.3: A state-space diagram for a three state system.

Continuous Markov

There is not a big difference between the discrete and the continuous Markov model. In the discrete there has to a transition inside the chain (could be to the same state) while in the continuous Markov model the time until the next transition is stochastic.

A state-space diagram for a three state system can be seen in Figure 2.2. That system will give a matrix, as in Equation 2.6.

$$A = \begin{pmatrix} -(\mu_1+\mu_2) & \lambda_1 & \lambda_2 & 0 \\ \mu_1 & -(\lambda_1+\mu_2) & 0 & \lambda_2 \\ \mu_2 & 0 & -(\lambda_2+\mu_1) & \lambda_1 \\ 0 & \mu_2 & \mu_1 & -(\lambda_1+\lambda_2) \end{pmatrix} \tag{2.6}$$

Mainly the long-run (steady state) probabilities are of interest in reliability calculations. Then is only the asymptotic solution which is of interest. The steady state equation is shown in Equation 2.7.

$$\mathbf{AP} = 0 \tag{2.7}$$

Since the system always has to be in one of the states the condition in Equation 2.8 is also valid.

$$\sum_{i=1}^{4} P_i = 1 \tag{2.8}$$

Expressions 2.7 and 2.8 from a set of equations with only one solution: the steady state probabilities. Solving the latter equations for the example will give the following solution:

$$P_1 = \frac{\lambda_1\lambda_2}{(\lambda_1+\mu_1)(\lambda_2+\mu_2)} \tag{2.9}$$

$$P_2 = \frac{\lambda_2\mu_1}{(\lambda_1+\mu_1)+(\lambda_2+\mu_2)} \tag{2.10}$$

$$P_3 = \frac{\lambda_1\mu_2}{(\lambda_1+\mu_1)+(\lambda_2+\mu_2)} \tag{2.11}$$

$$P_4 = \frac{\mu_1\mu_2}{(\lambda_1+\mu_1)+(\lambda_2+\mu_2)} \tag{2.12}$$

This gives the following mean duration and visit frequency for each state.
Mean duration of a visit

$$D_j = \frac{1}{\sum a_{ji}} \quad for \quad i \neq j \tag{2.13}$$

Visit frequency

$$F_j = P_j \frac{1}{D_j} \tag{2.14}$$

2.4.4 Monte-Carlo simulation

Evaluation techniques are of two main types: analytical and simulation. Using analytical evaluation techniques demands mathematical models that describe everything. For complex systems with a large dependencies the evaluation is not solvable analytically. By using simulation techniques, like Monte-Carlo, even larger complex systems can be solved. The Monte-Carlo methods, described in [5, 8, 9] are quite computer extensive but have some other advantages. The main advantage is handle of both deterministic and stochastic models and dependencies. The simulation can include almost anything that effects the system such as weather variations, human errors, planned shutdowns and interactions with other systems. Differences in the models due to the different external factors can easily be counted for. An example of a complex dependency in electric power systems is the following. The failure of a component (e.g. a transmission line or a generator) will lead to higher loading of some of the remaining components. If the loading gets too high this will lead to an increased failure rate of these components. As many large-scale blackouts are due to multiple failures, such dependencies are important to consider in a reliability study.

The main idea with the Monte-Carlo method is the simulation of realistic or "typical" simulations. By repeating the "typical" simulations the resulting distribution of any stochastic variable can be determined. The more repetitions the higher accuracy and a high amount of the repetitions is especially needed for rare events [5].

The Monte-Carlo methods are often used in complex mathematical calculations, stochastic processes simulations, medical statistics, engineering system analysis and reliability calculations [8].

For further studies of Monte-Carlo methods [9] is recommended.

2.5 Renewable Energy

The generation capacity now contains a third term (next to forced and planned unavailability): the fluctuations in the availability of the energy source. Such studies have been done already for large hydro installations, where the water level in the reservoir depends on the amount of rain or snow over the previous year or so. With wind and solar power the fluctuations affect the generation capacity even more.

The fluctuations in wind power are dependent on various non-human-controlled factors, e.g. different meteorological conditions. Some factors that affect solar power, that are also non-human-controlled, are time of the day, day of the year, water content in the air and cloud coverage.

When use of renewables it is important to investigate the individual potential in each kind of source get the maximum out of the sources. This will be discussed in more detail in the next chapter.

Chapter 3

Power System Models

To be able to do reliability calculations of isolated power systems are models needed for various components of the system. The models presented in this chapter are:

- Sun power generation model
- Water power generation model
- Wind power generation model
- Load model
- Storage model

The emphasis of the research has been on modelling solar and wind power. Therefore simpler models has been taken for the other components.

3.1 Sun power generation model

In this section a model for simulating six-minute mean values of global solar radiation without any geographical restrictions is proposed and discussed. This model only uses the geographical coordinates of the location and cloud coverage data as input. A method of generating cloud coverage data by using a discrete Markov model is also proposed.

Several models have been proposed for generation of global radiation. The random nature of global solar radiation is included in all proposals, but the way of implementing this in a model varies significantly. In [10, 11, 12] they model daily global solar radiation (thus the yearly variations) but a higher resolution of the simulation is needed for photovoltaic power generation in an autonomous electric power system. Such model would be applicable in a system with a storage capability higher than the daily load demand. The model of [10, 12] requires several years of solar radiation measurements, which are for most locations not available. The model proposed by [11] is adapted for clear sky conditions but the authors mentioned the importance of the cloud coverage. In [13] hourly radiation have been modelled but the model could be difficult to apply due to the data requirements. Monthly average values of global radiation are needed which can only be obtained from long time measurements. Another model is proposed in [14] the problem with the input of the model remains. A location-dependent factor is used which depends on the probability distribution of the solar radiation. This model can again only be used when a large amount of solar radiation data is available.

Outside the atmosphere the solar radiation can accurately be determined [15] and the atmosphere will induce the randomness [13]. The transmittivity of solar radiation in the atmosphere depends on various factors, e.g. humidity, air pressure and cloud type. A factor that has a great impact on the transmissivity is the cloud coverage [11, 16]. By assuming a deterministic relation between cloud coverage and hourly global solar radiation, the need for measurement of the latter disappears. Cloud observations can be used because of the simplicity of measuring, no expensive equipment is needed. The level of cloudiness is expressed in Oktas which describes how many eight parts of the sky that are covered with clouds [17]. By combining the solar radiation model with a model of simulating cloud coverage the simulation method could be even more suitable. The solar radiation distribution is expected to be similar in areas with similar climatological conditions [14]. That means that this method could be used when cloud observations are available for an area with similar climatological conditions. In reliability simulations for power systems without storage capacity, simulation data with higher resolution than one hour is needed in some cases. This is the case when short-duration interruptions (less then one half hour) are a concern.

3.1.1 Definitions

Oktas	The integer number of eighth parts of the sky which is covered with clouds.
Solar declination angle, $[\delta_s]$	The angle between the equator and the center of sun to center of earth line, see figure 3.1.
Elevation angle, $[\psi]$	The angle between the sun and the horizon.
UTC	Coordinated Universal Time, the reference time, other names are GMT (Greenwich Mean Time) and Zulu Z Time.
Global radiation	The total radiation to the earth include reflections from the clouds, positive towards the center of earth.
Net income radiation	The direct radiation from the sun.

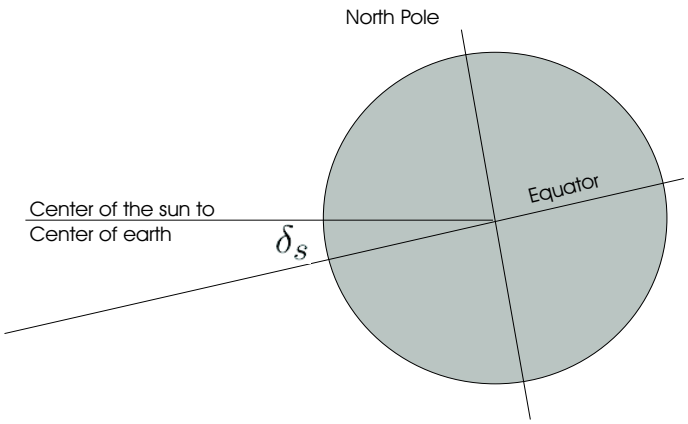

Figure 3.1: The solar declination angle [δ_s].

3.1.2 Astronomical and Meteorological relationships

The model consists of two parts, one deterministic and one stochastic. The deterministic part contains the astronomical effects while the meteorological effects are stochastic.

Astronomical effects are due to the earth orbiting around the sun and the rotation of the earth around its axis. The seasonal and daily variations can be described by equation 3.1 and 3.2 [15].

The equation for the seasonal effects 3.1, is an approximation under the assumption of circular orbit of the earth around the sun. This assumption is allowed because the excentricity is only 0.07 and the results are only used in stochastic ways. Equation 3.2 describes the daily effects and is dependent on the geographical location.

$$\delta_s \approx \Phi_r \cos\left[\frac{C(d-d_r)}{d_y}\right] \tag{3.1}$$

$$\begin{aligned} \sin\psi &= \sin\phi\sin\delta_s \\ &- \cos\phi\cos\delta_s\cos\left(\frac{Ct_{UTC}}{t_d} - \lambda_e\right) \end{aligned} \tag{3.2}$$

Where:

- δ_s Solar declination angle, [rad]
- Φ_r The tilt of the earth's axis relative the orbital plane of the earth around the sun, $\Phi_r = 0.409$ [rad]
- C $C = 2\pi$, [rad]
- d Day of the year, [days]
- d_r The day of the year at summer solstice, 173 (22 June) for non-leap years, [days]
- d_y Total number of days in one year, [days]
- ϕ Latitude of the location [rad]
- λ_e Longitude of the location [rad]

The adjustment to local time from Coordinated Universal Time (UTC) is needed when the model should be used for reliability calculations and then combined with loads.

Loads have often a high correlation with time and therefor it is necessary to work with local time.
The randomness in this simulation model for global solar radiation is introduced in the meteorological part of the model. The importance of the randomness in the atmosphere is also discussed in [13]. An empirically determined relationship between the global solar radiation and the cloud coverage, equation 3.3 was obtained by the authors of [16], after many years of cloud observations, solar elevation measurements and global solar radiation measurements. The obtained relationship reads as follows:

$$S = \left[\frac{a_0(N) + a_1(N) \sin\psi + a_3(N) \sin^3\psi - L(N)}{a(N)} \right] \tag{3.3}$$

S is the global solar radiation; the values of the constants $L(N), a(N)$ and $a_i, i = 0, 1, 3$ in equation 3.3 are given in Table 3.1.

Table 3.1: The empiric determined coefficients for (3.3)

N	a_0	a_1	a_3	a	L
0	-112.6	653.2	174.0	0.73	-95.0
1	-112.6	686.5	120.9	0.72	-89.2
2	-107.3	650.2	127.1	0.72	-78.2
3	-97.8	608.3	110.6	0.72	-67.4
4	-85.1	552.0	106.3	0.72	-57.1
5	-77.1	511.5	58.5	0.70	-45.7
6	-71.2	495.4	-37.9	0.70	-33.2
7	-31.8	287.5	94.0	0.69	-16.5
8	-13.7	154.2	64.9	0.69	-4.3

In figure 3.2 the global solar radiation is presented as a function of the solar elevation angle for the nine possible values of cloud coverage. Note that even for a fully clouded sky, a non-negligible part of the solar radiation reaches the solar panel (about 25%).

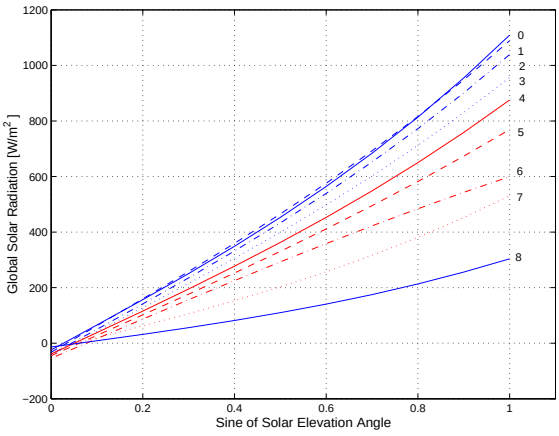

Figure 3.2: The relationship between global solar radiation and solar elevation angle for different cloud coverage. The number represents the cloud coverage level.

If the global radiation is below zero in 3.3 it should be set to zero according to equation 3.4. If the radiation is negative it is from the surface of the earth upwards. This radiation has another frequency spectrum and will not generate any power from solar panels. This situation will occur during night time and for low elevation angles.

$$\text{if} \quad \psi_i < 0 \quad \text{or} \quad S_i < 0 \quad \text{then} \quad S_i = 0 \quad \forall \quad i \tag{3.4}$$

By examining global solar radiation measurements it can be seen that the radiation varies within a one-hour period. This phenomena could be simulated by introducing a statistically varying term according to equation 3.5. This statistical term (ϵ) proposed to have the same distribution as the short duration variations seen in the measurements.

$$S_{stat} = S + \epsilon \tag{3.5}$$

The statistically varying term can be estimated through cross validation, the so-called "hold out method" proposed by [18]. The deviation from the hourly mean values for day time can be fitted to a normal distribution and the mean value and the standard deviation can be estimated. The mean value of the deviation was estimated to zero and the standard deviation to 40 W/m^2 for a set of data obtained at Säve Airport, close to Göteborg.

3.1.3 Results

To show some result of the global solar power model measured data obtained at Säve Airport (57.72 °N, 11.97 °E), close to Göteborg, was used. The data series consists of six-minute mean values of the global solar radiation and cloud coverage every three hour for 27 year. Hourly values of the cloud coverage were obtained through linear interpolation. The interpolated values were rounded to the nearest integer to correspond to a cloud coverage value.

To be able to see the difference between the different oktas, the solar radiation during a whole year has been calculated with a constant oktas. The maximum value, of the solar radiation for each day is displayed for each oktas in figure 3.3.

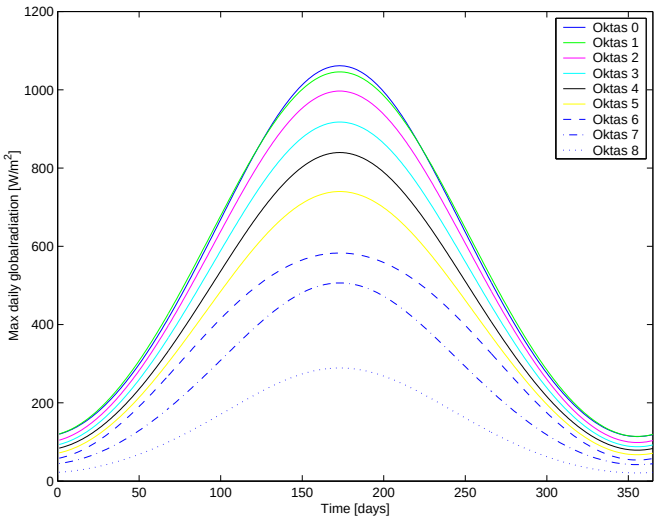

Figure 3.3: Global solar radiation during one year for different oktas.

Figure 3.4 shows the maximum value of global solar radiation each day during one year, as measured at Säve airport in Göteborg. As expected, the measured curve fluctuates between the curve for oktas 0 (no clouds) and oktas 8 (fully clouded) in figure 3.3.

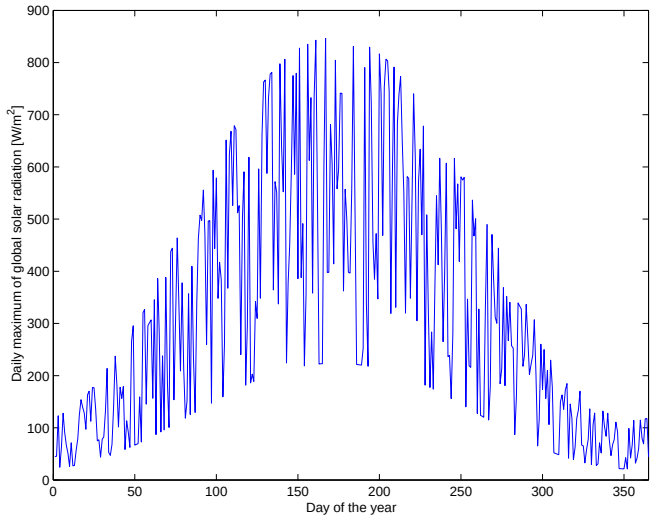

Figure 3.4: Calculation of the solar radiation for a year in Göteborg.

In figure 3.5 the global solar radiation, both measured and calculated, are shown for a few days in February. The calculated values where obtained by applying equation 3.3 to the interpolated 1-hour values of the observed cloud coverage.

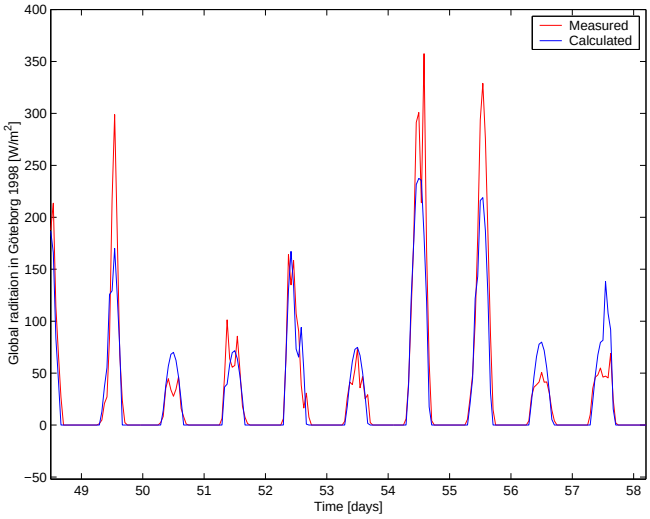

Figure 3.5: Solar radiation for Göteborg from 18th to 27th of February.

In table 3.2 the mean values and standard deviations for 1998 and 1999 are compared.

Table 3.2: Comparison of measured and simulated solar radiation

	Measured		Calculated		Difference [%]	
Year	Mean	Std	Mean	Std	Mean	Std
1998	97	172	103	184	+6	+5
1999	105	183	109	191	+4	+4

Figure 3.6 shows a comparison between measured and calculation of the statistically varying term. The statistically varying term calculated values were added the hourly mean values of the measured data to eliminate the hourly variations. This was done to obtain comparable curves in the sense of six minutes values.

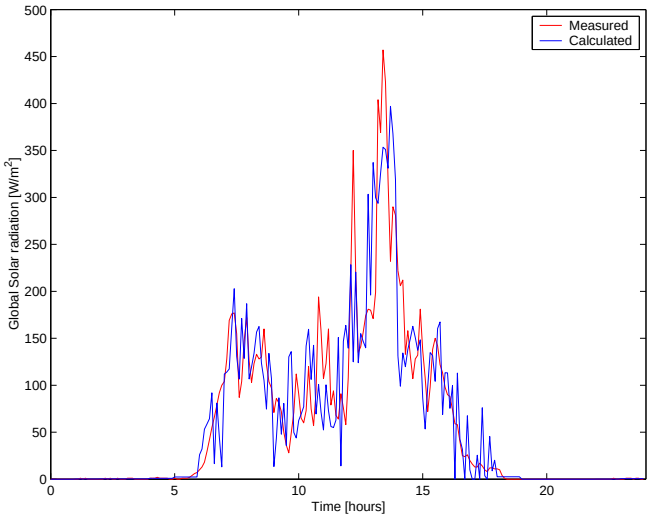

Figure 3.6: Comparison of six minute values for a day in September 1999.

3.1.4 Cloud simulations

To make the model less dependent on observed cloud coverage data and thereby make it more available for power system reliability calculations a model for simulate cloud coverage data is developed. To use simulation techniques like Monte-Carlo many years of global solar radiation data is needed to get some statistic certainties. A Markov model is proposed to generate cloud coverage data from which global solar radiation can be obtained. A Markov model was chosen because of its easiness and whereas it still allows dependencies to be accounted for. The transition probabilities in the Markov model were obtained from measured values in the perhaps most intuitive way:

$$\hat{\lambda}_{ij} = \frac{f_{ij}}{\Sigma_{k=0}^{8} f_{ik}} \tag{3.6}$$

Where:

$\hat{\lambda}_{ij}$ Is the estimated transitions probability
f_{ij} The number of transitions from cloud coverage level i to level j
f_{ik} The number of transitions from cloud coverage level i to level k

By using 27 years of cloud coverage data the transition probabilities could be determined. The results are shown in matrix form below.

$$\hat{\Lambda} = \frac{1}{100} \begin{pmatrix} 54 & 22 & 7.1 & 4.7 & 2.7 & 2.3 & 1.7 & 2.6 & 2.6 \\ 16 & 46 & 14 & 9.1 & 4.3 & 3.7 & 3.2 & 3.0 & 1.5 \\ 7.0 & 25 & 23 & 15 & 8.8 & 7.2 & 6.2 & 5.4 & 2.2 \\ 3.8 & 13 & 18 & 20 & 13 & 11 & 9.0 & 9.1 & 3.4 \\ 2.2 & 8.5 & 12 & 16 & 16 & 14 & 13 & 13 & 4.2 \\ 1.5 & 5.1 & 8.1 & 12 & 13 & 17 & 19 & 18 & 6.2 \\ 1.0 & 3.0 & 5.2 & 7.4 & 9.5 & 14 & 22 & 28 & 9.5 \\ 0.6 & 2.0 & 2.3 & 3.0 & 3.9 & 6.3 & 11 & 50 & 20 \\ 0.5 & 0.7 & 0.8 & 1.1 & 1.3 & 2.0 & 3.8 & 14 & 76 \end{pmatrix} \tag{3.7}$$

This way of simulating will generate cloud coverage data with the same time step as the data used for input. The data used for this model have a time step of three hours which means that if this model is used it will generate simulated cloud coverage data with a time step of three hours.

As wether patterns are seasonally-dependent, the transition probabilities are also expected to be different for different times of the year. Having 27 years of cloud coverage data available it was possible to study the seasonal-dependency of the matrix with transitions probabilities. To investigate the dependencies of the time of the year, the year was split up into 12 periods (months). A transition probability matrix was determined for each period, see figure 3.7 to 3.15. Figure 3.7 shows the nine transition probabilities from state zero to all other eight states and how they depend on the time of the year. The other figures, up to figure 3.15 show the same from state one, two, three, four, five, six, seven and eight. Note the difference in vertical scale.

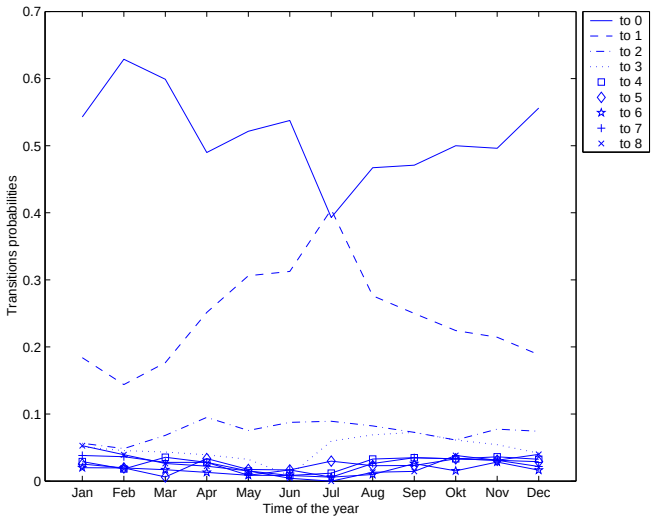

Figure 3.7: The variations of the transition probabilities, from state 0, over a year.

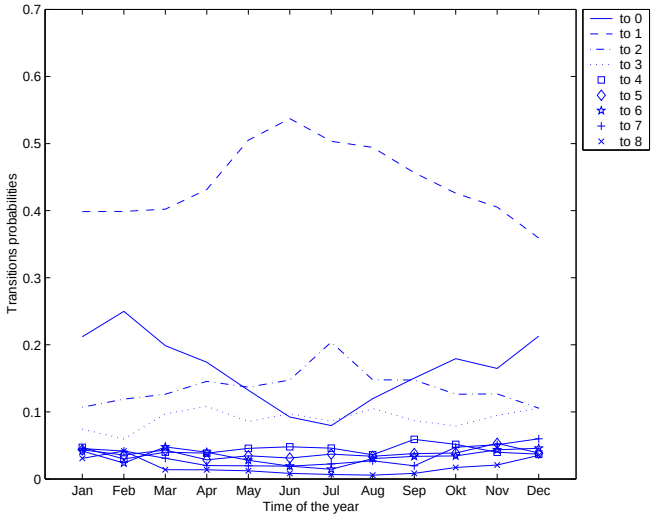

Figure 3.8: The variations of the transition probabilities, from state 1, over a year.

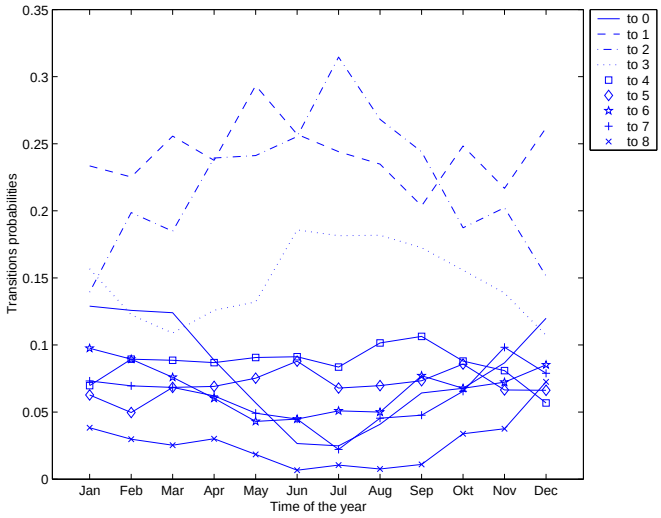

Figure 3.9: The variations of the transition probabilities, from state 2, over a year.

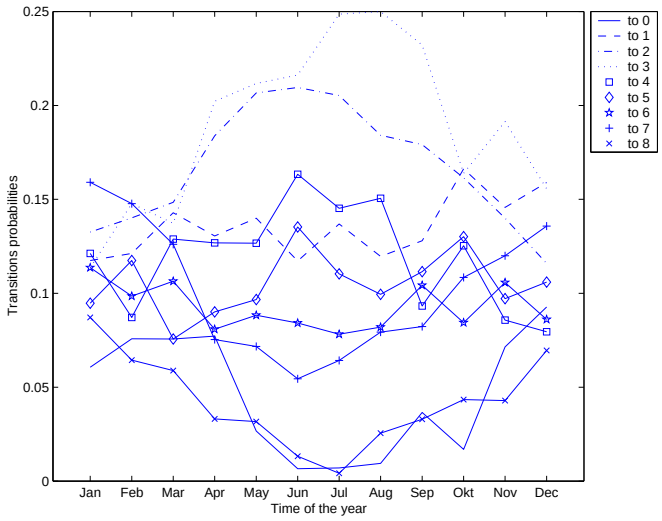

Figure 3.10: The variations of the transition probabilities, from state 3, over a year.

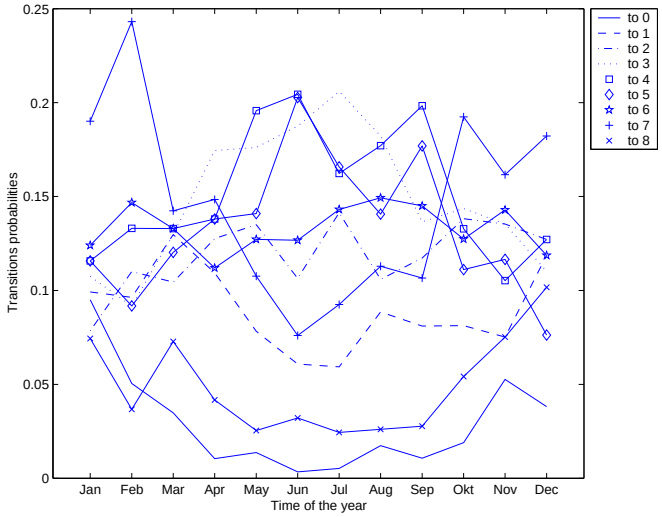

Figure 3.11: The variations of the transition probabilities, from state 4, over a year.

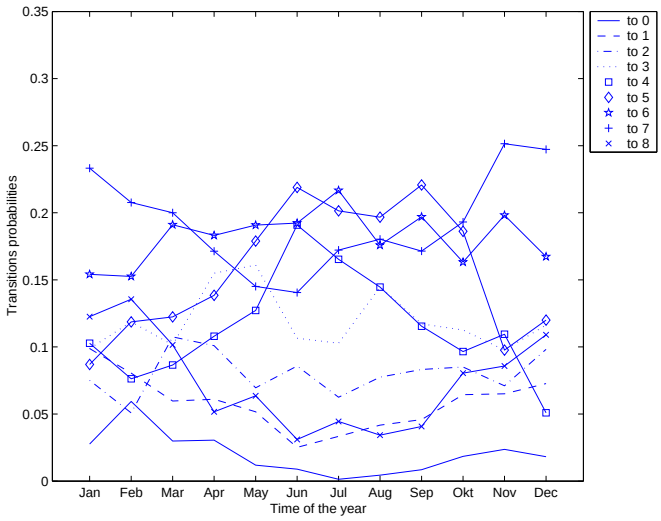

Figure 3.12: The variations of the transition probabilities, from state 5, over a year.

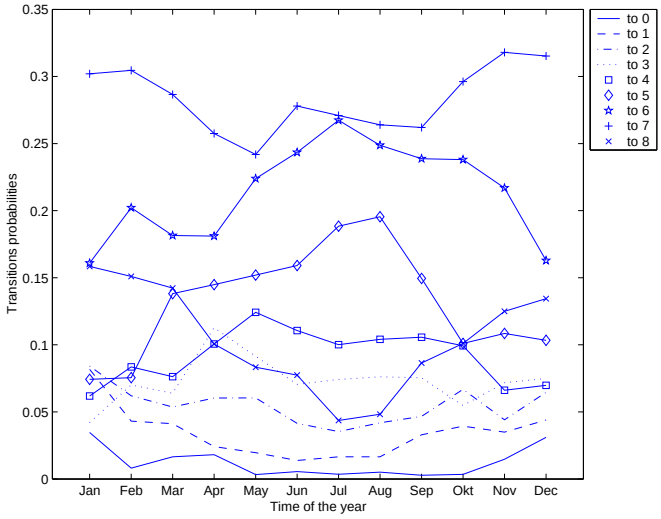

Figure 3.13: The variations of the transition probabilities, from state 6, over a year.

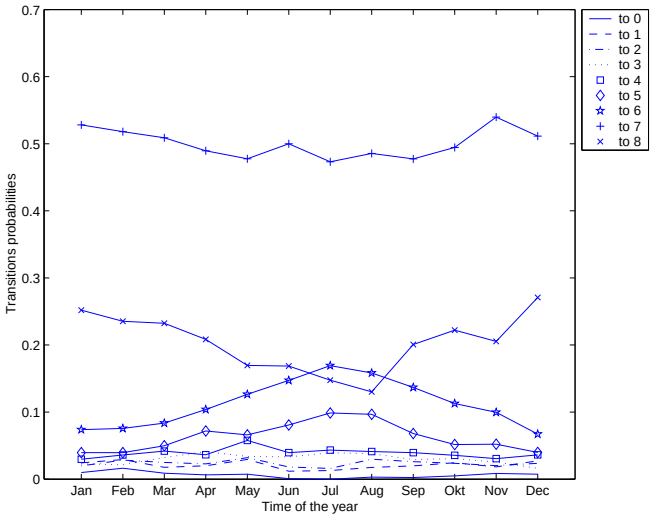

Figure 3.14: The variations of the transition probabilities, from state 7, over a year.

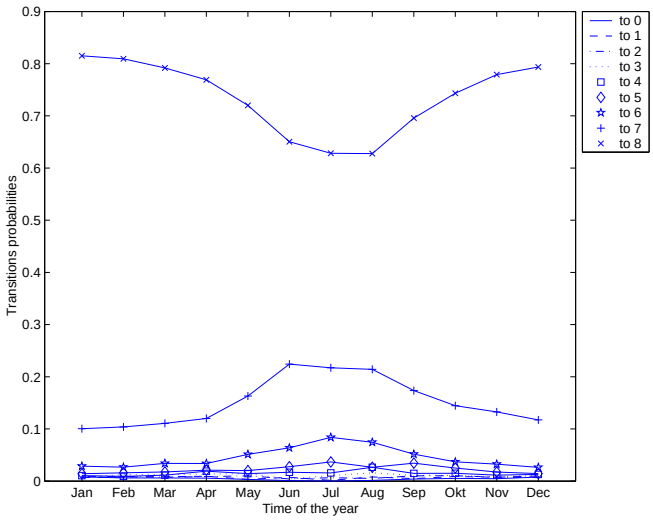

Figure 3.15: The variations of the transition probabilities, from state 8, over a year.

It can easily be seen that the transition probabilities are not constant during a year but using twelve different transition matrices would make the model unnecessary complicated. The year was divided into two parts, summer and winter, to account for the seasonal effects. The summer period is between April and September and the rest of the year was considered winter. In figure 3.16 shows the three most varying transition probabilities. The dotted line represents transition probability from state 0 to 1 while the dashed and the solid lines shows the transitions probabilities from 7 to 8 and 8 to 8, respectively.

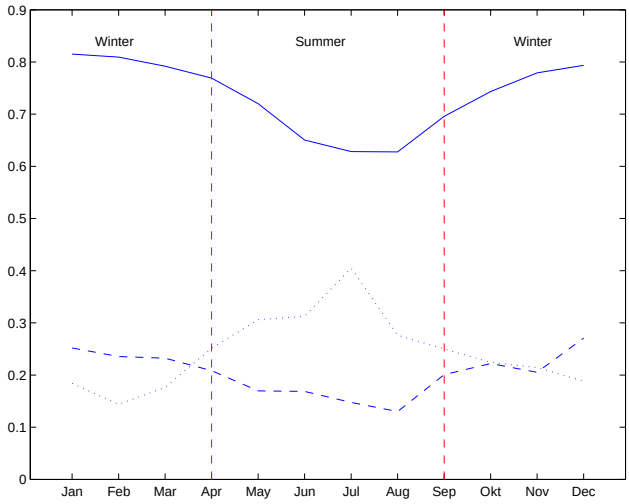

Figure 3.16: The winter and summer period and three transitions probabilities.

The resulting transition probabilities are for the summer period:

$$\Lambda_s = \frac{1}{100}\begin{bmatrix} 49 & 29 & 8.41 & 4.5 & 2.3 & 2.4 & 13 & 2.0 & 1.3 \\ 12 & 49 & 15 & 9.4 & 4.5 & 3.3 & 2.7 & 2.1 & 0.85 \\ 4.9 & 25 & 26 & 17 & 9.3 & 7.4 & 5.3 & 4.3 & 1.3 \\ 2.5 & 13 & 20 & 23 & 14 & 11 & 8.6 & 7.1 & 2.2 \\ 0.93 & 7.8 & 12 & 18 & 18 & 16 & 14 & 10 & 2.9 \\ 0.89 & 4.1 & 7.9 & 13 & 15 & 20 & 19 & 16 & 4.2 \\ 0.57 & 2.0 & 4.7 & 8.2 & 11 & 17 & 24 & 26 & 7.0 \\ 0.27 & 1.7 & 2.3 & 3.6 & 4.3 & 8.1 & 14 & 49 & 17 \\ 0.26 & 0.50 & 0.78 & 1.2 & 1.7 & 2.7 & 5.5 & 18 & 70 \end{bmatrix} \tag{3.8}$$

and for the winter period:

$$\Lambda_w = \frac{1}{100}\begin{bmatrix} 57 & 18 & 6.3 & 4.8 & 3.0 & 2.2 & 2.0 & 3.0 & 3.6 \\ 20 & 40 & 12 & 8.6 & 4.1 & 4.2 & 4.0 & 4.6 & 2.5 \\ 11 & 24 & 18 & 13 & 8.0 & 6.8 & 7.9 & 7.5 & 3.7 \\ 6.2 & 15 & 14 & 15 & 11 & 10 & 10 & 13 & 5.8 \\ 4.6 & 10 & 12 & 12 & 13 & 11 & 13 & 18 & 6.7 \\ 2.8 & 7.1 & 8.3 & 11 & 8.9 & 13 & 17 & 22 & 10 \\ 1.6 & 4.6 & 6.2 & 6.3 & 7.7 & 10 & 20 & 30 & 13 \\ 0.91 & 2.3 & 2.3 & 2.5 & 3.5 & 4.6 & 8.6 & 52 & 23 \\ 0.57 & 0.79 & 0.82 & 1.0 & 1.2 & 1.7 & 3.0 & 12 & 79 \end{bmatrix} \tag{3.9}$$

The method of using two matrices, summer and winter, is used for the reliability calculations in this thesis.

3.1.5 Solar cells

There are today many different techniques of convert solar radiation to electric energy. In this chapter a selection of techniques of solar cells are presented [19].

Silicon Cells

There are three different kinds of silicon solar cells, mono-crystalline, poly-crystalline and thin film.

Mono-crystalline solar cells are made from extremely pure silicon. That silicon was originally made for the electronic industry and therefore extremely pure and therefore expensive. The efficiency is high but the process to purify (e.g. Czochralski) is very expensive and time consuming. Until recently this kind of solar cells has been the technique behind the majority of installed solar cells.

The idea behind poly-crystalline solar cells are that the silicon consists of small grains of mono-crystallines and therefore does not need the extreme purity as for the mono-crystalline cells and thereby reduces the cost of manufacturing. The efficiency will be lower due to the impurity. However, solar panels with poly-crystalline can be made more efficient than mono-crystalline because the poly-crystalline can be made quadratic

and thereby have a higher effect area per panel. Poly-crystalline is also be called semi-crystalline or multi-crystalline.

Mono-crystalline and poly-crystalline cells need to have a thickness of several hundred micrometers to ensure absorption of the photons. If the silica is combined with advanced light trapping techniques the layers of around 20 μm can be used. These are called poly-crystalline thin films and the cells need to be supported by ceramic substrates. However, these cells are thicker then other thin film cells and are therefore sometimes called "thick film cells". The advantages of these solar cells are higher efficiency than poly-crystalline cells and lower production cost due to low material cost and low processing cost.

Another type of silicon-based solar cells are amorphous silicon (a-Si) solar cells. In an a-Si cell the atoms are less structured then in crystalline cells and then lose bonds will occur which are then use for the doping. A-Si is less expensive to produce because thinner layers and lower temperature in manufacturing process. The panels are thereby more flexible and can be formed into almost any shape. A-Si is less effective than crystalline. A disadvantage of a-Si is that it is degrading due to sunlight.

III-V

Solar cells can be made from other materials then silicon. It are mainly combination of materials from and around group III to V in the periodic table. Useful combinations have been found in Gallium/Arsenic, Copper/Indium/Diselenide and Cadmium/Tellurium.

Gallium/Arsenic (GaAs) has a crystal structure close to silicon but consists of alternating gallium and arsenic atoms. GaAs cells have a high efficiency because the crystal has a wider band gap then silicon: closer to the optimum of absorbing the energy in the terrestrial solar spectrum. It has also a high light absorbtion coefficient, so that only a thin layer of material is needed. The GaAs cell can operate at relatively high temperature which makes them useful for concentrators. Despite this advantages the techniques is not often used because of high cost not only in production but also in material. Since the efficiency is high the GaAs cells have been used for space applications.

Copper/Indium/Diselenide (DIS) is a another thin film technology. DIS has a high efficiency and almost no degradation due to sunlight but Indium is a relative expensive material and the manufacturing involves high toxic substances which cause server health hazards in case of an industrial accident.

Cadmium/Tellurium (CdTe) is a low cost cell with no degradation and with useable efficiency. The main problem is the cadmium which is highly toxic. Restrictions needs to be taken during the whole lifetime of the cell from production to disposal.

Multi-junction

The benefits from different solar cells can be combined by using multi-junction solar cells. Two or more cells are "stacked" onto each other. Cells for different part of the frequency spectrum can be combined. For example a-Si on top for the higher part of the spectrum and then another thin film a-Si with a band gap to absorb the lower part of the spectrum. This increases the efficiency but also the cost. A cell with two different layers is often called a tandem device.

Concentrating

One of the problem with the solar energy is the lack of solar radiation. By concentrating the radiation the solar cells can be used more efficient. There are different ways of concentrating the radiation.

The most obvious and the mostly used way of concentrating radiation is with mirrors and lenses. By controlling the mirrors and lenses with motors the sun can be followed.

Another method, still under development, is using a fluorescent concentrator. It absorbs light in a wide spectrum and emits in a narrow bands of wavelengths. By choosing a solar cells especially designed for the band the efficiency can be high.

Polymeric

Another technology that is today still under development are polymer solar cells. The development is still in an early stage of development. The largest problems are low efficiency and bad stability. New materials and improved control of the device architecture are needed. The main advantages are use of environmental friendly materials and inexpensive production, since the solar cells can be "printed" on almost any material surface [20].

Efficiencies of different solar cells technologies

Table 3.3 gives the maximum efficiency of different solar cells [21]. The values are achieved in test laboratory at global AM 1,5 spectrum (1000 W/m^2) except for the polymeric cells where 100 mW/cm^2 was used.

What kind to choose for different situations is not discussed in this thesis. The most important factor for choosing solar cells are in most cases the economical aspects which are not part of this thesis.

For all the calculations the solar panels in this thesis are considered ideal except for the efficiency which is assumed to be only 6% to make sure not to overestimate the benefits of solar cells.

Table 3.3: An overview of efficiency of different solar cell technologies.

Type	Efficiency [%]
Silicone	
Si(mono)	$24,7 \pm 0,5$
Si(poly)	$19,8 \pm 0,5$
Si(film)	$10,1 \pm 0,2$
a-Si	$16,6 \pm 0,4$
III-V	
GaAs(mono)	$25,1 \pm 0,8$
DIS	$12,5^a$
CdTe	$16,5 \pm 0,5$
Multi-junction	
GaInP/GaAs[b]	30,3
GaInP/GaAs/Ge[c]	$32,0 \pm 1,5$
Polymeric[d]	2,5

[a]: Value from [19].
[b]: example of Two-cell stack (tandem).
[c]: example of Three-cell stack.
[d]: Highest achieved value according to [20].

3.2 Hydro power generation model

Today there is a large interest of using small scale hydro power generation by using so-called micro turbines. The model used in this thesis consists of a constant water flow and a small reservoir. A schematic of the system is shown in figure 3.17: P_{river} is the power in the incoming water flow, ϵ_w is the stored energy in the reservoir, P_{water} is the output power from the hydro model and P_{over} is the wasted power due to an overfull reservoir.

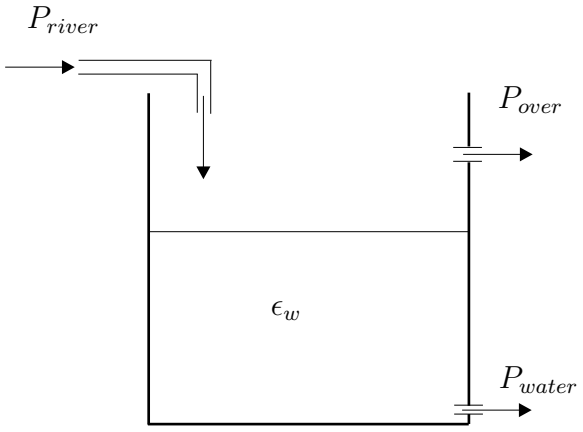

Figure 3.17: Schematic figure of water generation system.

In equation 3.10 the energy available in storage water is presented where ρ_{water} is the density of water (approx. $1000kg/m^3$), V is the volume of the water, g is the gravity constant (approx. $9.80m/s^2$) and h is the mean height of the water in the reservoir.

The height of the reservoir was assumed to be $5m$ and that gives a mean height at $2.5m$.

$$P_{water} = \frac{\rho_{water} V g h}{3.6 \cdot 10^6} \tag{3.10}$$

The complete system was assumed to have a efficiency of just 50 % to not overestimate the influence of the water generation. In all other senses the hydro power model was considered ideal.

3.3 Wind power generation model

In this section a model is proposed for generating simulated power output time series from a wind turbine. The model is based on Markov models,"one-seventh power law equation" [3] and data from a conventional wind turbine [22]. The model includes a possibility of adapting to different geographic areas with different yearly mean values.

In the area of wind power modelling many research years have been spent to make models and forecast for wind power generation. The methods vary quite a lot but all agree on statistical variations with some correlations between following factors and the great importance of field measurement as basis of the simulation. The need for describing the wind power model statistically is discussed in [23]. It is well known that the wind speed distribution can be fitted to a Rayleigh distribution or the more general Weibull distribution. This has been done in [23, 24, 25, 26] but differences are in including the correlation between two consecutive values. Measurements are needed to determine this correlations. These models are quite complicated and therefore need large computational resources and that is not practical when the simulation is just a small part of the system simulation. Some of the models are adapted to wind farms [4, 25] and that adds more complexity to the problem. The wind direction has a greater importance because of the shading effects of the other wind turbines in the farm. Due to the greater complexity the model while be more extensive. For simulation of single wind turbines shading generally not included. In [27, 28] Markov models are used to simulate the values. A great advantage of using a Markov model is that it is not distribution dependent and it is easy to use. In [27] Markov models are coupled to simulation of wind direction. A combination of simulating wind speed and wind direction is very useful because there is normally a strong correlation between speed and direction of the wind. In coastal areas (on land), where it could be beneficial to install wind turbines, there are normally great differences between land and sea wind. To determine the model factors, measurements of both wind speed and wind direction are needed. By using only one matrix the wind speed intervals must be large to still have a manageable number of elements. In [28] the authors have proposed two different models, both based on the Markov theory. The first model is a Markov model with 19 states. The transition probabilities were calculated using measured wind speed data. This method had only correlation between two consecutive values. In the second model the wind speed is divided into three regimes, weak (states 1-7), medium (states 4-12) and strong (states 11-19). Overlapping is allowed to enable single high/low values in one regime. A start regime is selected and the time for spending in each regime is

determined using the original measured data. The length of time in each regime is stochastic variable. On average the wind speed is 1/3 of time in the weak-wind regime, 1/2 of time in medium-wind regime and 1/6 of time in the strong-wind regime. The step of the simulations is one hour. According to the authors a further split is needed in to three seasons, winter (120 days), midseason (77 days) and summer (168 days). In comparison with measured data the simulations methods had similar mean values and distributions.

3.3.1 Obtaining the measured data

As input for the model data were used that were obtained at Näsudden, Sweden.(57°4'N 18°13'E) Näsudden is close the very south of Gotland. Näsudden is and has been for a long time used for studies of wind turbines. One of the world's first 2 MW wind turbines was installed in this location. More information regarding the wind turbines at Näsudden can be found in [29].

Figure 3.18: Map of Gotland, Näsudden is marked.

The data used for determine the Markov models are measured at a height of ten meters and were of contentiously measured ten minutes mean values. The measurements were conducted by the Department of Earth Sciences at the University of Uppsala 1992 until 1994.

The mean values of the years from 1992 until 1994 were quite average years, as can be seen in figure 3.19, where the yearly mean values are shown, 1992 until 1994 were ordinary years.

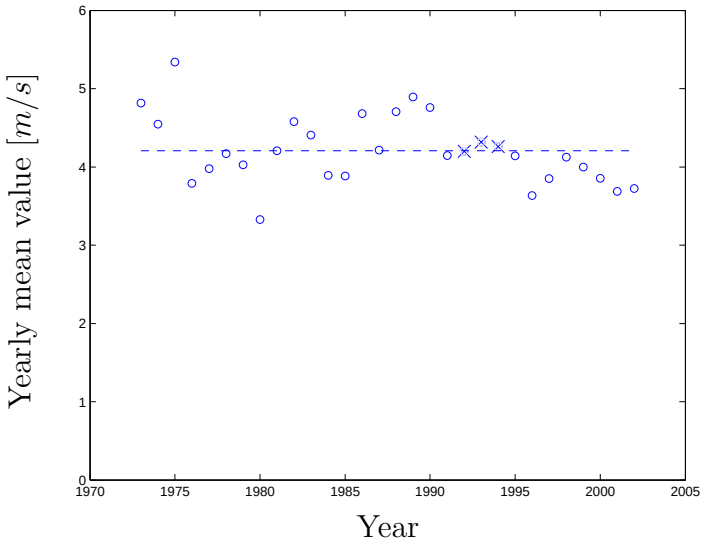

Figure 3.19: The yearly mean values of 30 years.The dashed line shows average over the whole period.

3.3.2 Simulation using Markov Models

Generating artificial wind speed data can be done by using Markov models. In this section a simulation model is proposed based on two Markov Models. One Markov model for hourly mean value below yearly mean and one for values above yearly mean. By doing this split up into two models the common behavior of the wind measurement, looking like there are two different mean values and the is randomly change between these two levels. This phenomenon could be explained by wind from different directions. A common location for wind turbines are in coastal areas often quite close to the water, for example see the wind turbine site in section 3.3.1. In this kind of areas there are often quite large differences between wind from the water and wind from land. Figure 3.20 shows 10 minutes mean values for 20 days in 1992 and the two level behavior can easily be seen. The levels are approximately 2 m/s and 6 m/s.

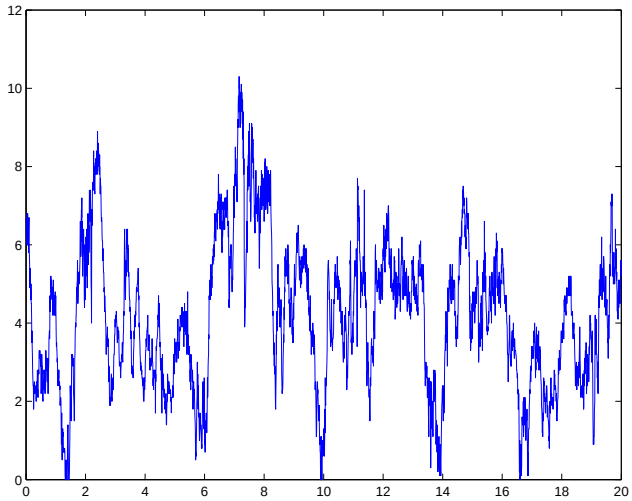

Figure 3.20: Wind speed measurements for 20 days in 1992.

To make the simulation more adaptable for generation of wind speed data the yearly

mean value was normalized to one. This can be done without change the distribution of wind speed which is together with the dependencies, for this case the interesting information. The Weibull distribution is most distribution fitted to wind data and the wind speed is in general considered according to this distribution [23, 24, 25, 26, 3]. By normalizing the wind speed data the data could easily be adapted to any location by scaling with the yearly mean wind speed value with the same distribution as the original wind speed series.

By using measured wind speed data as input for the model it was possible to determine the transition probability matrices for the Markov models. The two models were defined as if the last hourly mean value was above or below the yearly mean value. In the low wind Markov model it is necessary to allow for some occasional high values because high wind squalls exists. Low wind squalls also exist in the high wind so the high wind model needs to take this in to account. The low wind model was discretized into 9 levels while for the high wind model 14 levels were used. The higher number of levels for the high wind model is because large span of wind speeds. The mean value for each level in the model was chosen so the yearly mean values of the simulated values would still be one. The intervals and mean, respectively for each level in the models are presented in table 3.4.

Table 3.4: The discretization of the wind speed data for the Markov models.

	Low wind		High wind	
Level	Interval $[m/s]$	Mean value $[m/s]$	Interval $[m/s]$	Mean value $[m/s]$
1	< 0.1	0.0325	< 0.7	0.5777
2	0.1-0.3	0.2230	0.7-0.9	0.8450
3	0.3-0.5	0.4090	0.9-1.1	1.0226
4	0.5-0.7	0.5989	1.1-1.3	1.2010
5	0.7-0.9	0.7984	1.3-1.5	1.3922
6	0.9-1.1	0.9772	1.5-1.7	1.5890
7	1.1-1.35	1.1708	1.7-1.9	1.7898
8	1.35-1.75	1.4651	1.9-2.1	1.9908
9	> 1.75	2.1356	2.1-2.3	2.1913
10			2.3-2.5	2.3859
11			2.5-2.7	2.5862
12			2.7-2.9	2.7825
13			2.9-3.25	3.0308
14			> 3.25	3.3892

The transition matrices can be estimated in many ways, the most intuitively is:

$$\hat{\lambda}_{ij} = \frac{f_{ij}}{\Sigma_{k=1}^{n} f_{ik}} \tag{3.11}$$

where $\hat{\lambda}_{ij}$ is the transition rate from state i to state j; f_{ij} is the number of transitions from state i to state j in the input data set and n is the number of states in the each

of the models.

In the two Equations 3.12 and 3.13 any transition probability that was calculated with lower than twelve samples was considered statistically not relevant [30]. By applying discretization and equation 3.11 the following transition matrices are obtained:

$$\hat{\Lambda}_l = \frac{1}{100} \cdot \begin{bmatrix} 65 & 32 & 2.9 & 0 & 0 & 0 & 0 & 0 & 0 \\ 7.8 & 67 & 24 & 0.78 & 0 & 0 & 0 & 0 & 0 \\ 0.13 & 8.6 & 75 & 16 & 0.40 & 0.08 & 0 & 0 & 0 \\ 0 & 0.14 & 12 & 74 & 14 & 0.42 & 0 & 0 & 0 \\ 0 & 0 & 0.21 & 14 & 71 & 14 & 0.45 & 0 & 0 \\ 0 & 0 & 0 & 0.47 & 24 & 68 & 6.8 & 0.16 & 0 \\ 0 & 0 & 0 & 0 & 2.3 & 38 & 55 & 4.6 & 0 \\ 0 & 0 & 0 & 0 & 0 & 0 & 0 & 100 & 0 \\ 0 & 0 & 0 & 0 & 0 & 0 & 0 & 0 & 100 \end{bmatrix} \tag{3.12}$$

$$\hat{\Lambda}_h = \frac{1}{100} \cdot \begin{bmatrix} 100 & 0 & 0 & 0 & 0 & 0 & 0 & 0 & 0 & 0 & 0 & 0 & 0 & 0 \\ 7.6 & 50 & 39 & 3.1 & 0 & 0 & 0 & 0 & 0 & 0 & 0 & 0 & 0 & 0 \\ 0.28 & 7.6 & 68 & 24 & 0.84 & 0 & 0 & 0 & 0 & 0 & 0 & 0 & 0 & 0 \\ 0 & 0.37 & 18 & 65 & 15 & 0.76 & 0 & 0 & 0 & 0 & 0 & 0 & 0 & 0 \\ 0 & 0 & 0.65 & 22 & 59 & 17 & 0.67 & 0 & 0 & 0 & 0 & 0 & 0 & 0 \\ 0 & 0 & 0 & 1.3 & 22 & 60 & 17 & 0.71 & 0 & 0 & 0 & 0 & 0 & 0 \\ 0 & 0 & 0 & 0 & 1.3 & 25 & 58 & 15 & 0.78 & 0 & 0 & 0 & 0 & 0 \\ 0 & 0 & 0 & 0 & 0 & 1.8 & 26 & 55 & 16 & 1.0 & 0 & 0 & 0 & 0 \\ 0 & 0 & 0 & 0 & 0 & 0 & 2.0 & 27 & 52 & 17 & 1.3 & 0 & 0 & 0 \\ 0 & 0 & 0 & 0 & 0 & 0 & 0 & 3.5 & 30 & 49 & 16 & 1.6 & 0 & 0 \\ 0 & 0 & 0 & 0 & 0 & 0 & 0 & 0 & 5.4 & 35 & 47 & 13 & 0 & 0 \\ 0 & 0 & 0 & 0 & 0 & 0 & 0 & 0 & 0 & 0 & 37 & 45 & 18 & 0 \\ 0 & 0 & 0 & 0 & 0 & 0 & 0 & 0 & 0 & 0 & 5.0 & 29 & 61 & 9.8 \\ 0 & 0 & 0 & 0 & 0 & 0 & 0 & 0 & 0 & 0 & 2.9 & 2.9 & 34 & 57 \end{bmatrix} \tag{3.13}$$

Through use of equations 3.6-3.13 simulated wind speed data is obtained with a yearly mean value of one. This can be seen i figure 3.21 where the result of ten independent simulations are shown. Each simulation had a length of 100 000 values and the mean value was 0.998. Each simulation started at mean value and in the low wind model but other simulations that started in the high wind model did not show any significant change in the result. The transitions between the low and high models occurs when the mean value for the last hour passes 1.0.

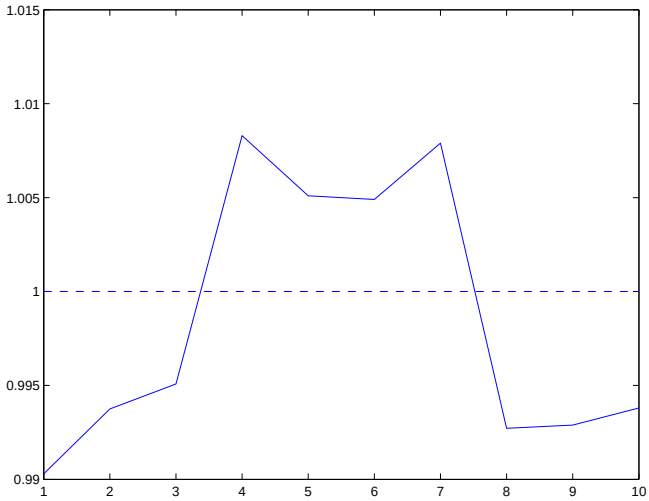

Figure 3.21: Mean value of ten simulations.

Since the model is normalised according to the mean value location specifics could be included in the model by its yearly mean value. If the simulated wind speed data is multiplied with the yearly mean value of the desired location artificial wind speed data can be obtained. The data has the same distribution as the input data but with the local yearly mean value.

Figures 3.22 and 3.23 shows measured and simulated wind speed data series. Both the series are normalized with mean value to one and are over a period of 2 months (8640 values). In the figures the similarity is obvious.

The resemblance of Figures 3.22 and 3.23 are only statistically. The two different levels, earlier mentioned, can be seen in both but the latter one is more edged because of the discretization. The more edged appearance makes a small difference but it is unavoidable if the states should kept at a reasonable number.

3.3.3 Wind speed variations with height

The wind speed vary at different height and that is a well known fact. Measuring wind speed at many different heights are in most cases unpractical because you normally do not at what height you are interested in. By using an relationship between different heights a measurement at a reference height is only needed. One common used relationship is the power law also known as ”one-seventh power law equation” [3] and it can also be known as Justus’ formula [31] and can be seen in equation 3.14.

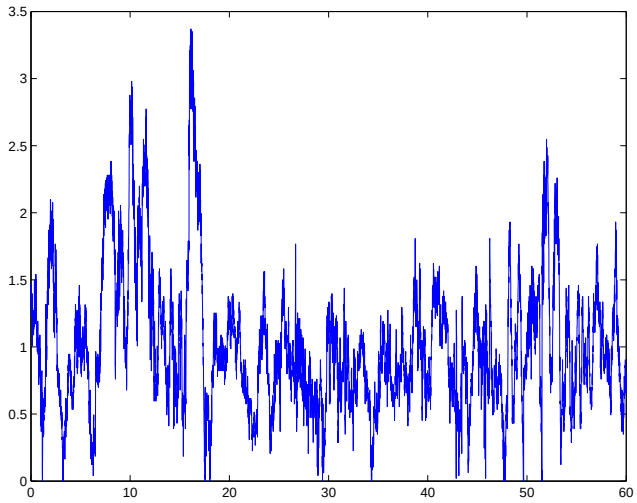

Figure 3.22: Two months of measured wind speed data normalized to mean value of one.

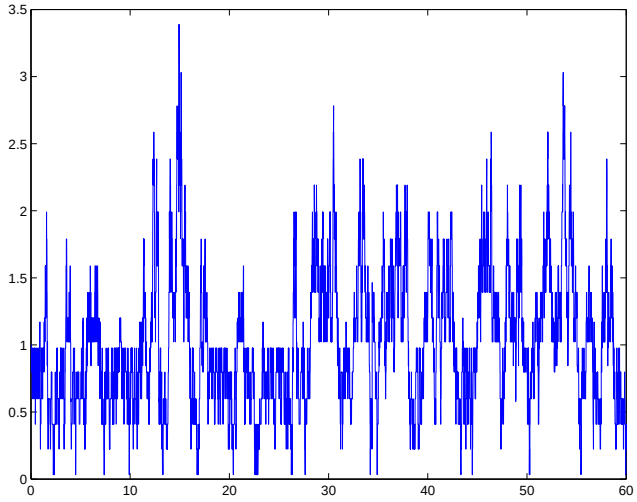

Figure 3.23: Two months of simulated wind speed data normalized to mean value of one.

$$\frac{v(z_2)}{v(z_1)} = \left(\frac{z_2}{z_1}\right)^{\alpha} \tag{3.14}$$

In equation 3.14, z_1 is the height of the measurements and z_2 is the height where the wind speed estimation is desired. $v(z_1)$ and $v(z_2)$ are wind speeds at height z_1 and z_2, respectively. α is the wind profile constant and is dependent on various factors e.g. height, wind speed, time of the day, season of the year, nature on the terrain and temperature. In [3] the authors have proposed a linear logarithm relationship, equation 3.15, to determined α and it is used in this model.

$$\alpha = a - b \cdot log_{10} u(z_1) \tag{3.15}$$

Daytime are typical values or a and b 0.11 and 0.061 and for nighttime 0.38 and 0.209. Time considered as daytime are from 6.00 to 19.50 and the rest of the day is considered

nighttime. In Figure 3.15 is the relationship shown between the wind profile coefficient and wind speed.

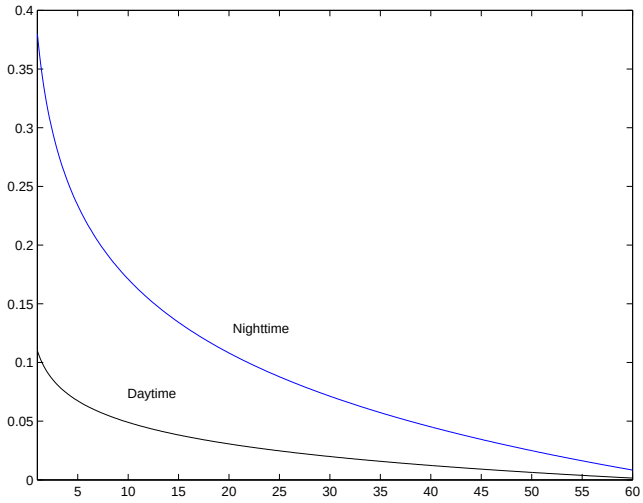

Figure 3.24: Wind profile coefficient α as a function of wind speed at z_1.

3.3.4 Wind Turbine

There are many different ways of converting wind energy into electric energy. There are different types of wind turbines. The classical windmill has been used since the ninth century. The windmills were used mainly in agriculture and another well-known application of windmills was in draining the polders in The Netherlands whereas today wind turbines are used to generate electricity for any purpose. This in large part due to the possibility of transporting electrical energy over large distances and thus allowing any application. The wind turbines of today exists in a wide range of sizes, from less then 10 kW and up to offshore wind farms with tens of wind turbines of several MW each.

The design of small wind turbine differs much from large turbines. Small turbines are mostly direct-driven machines with variable speed and permanent magnets. The aerodynamic profiles differs also and since manufacturers of wind turbine have a less interest in small turbines. The wing-profile of small turbines is less developed and they are therefore less effective. A small turbines requires a higher rotor speed to be able to achieve high reliability and low maintenance.

Large wind turbines were earlier designed according to the Danish Concept with fixed speed, stall regulation and asynchronous generator. However this concept is more and more replaced by newer technology. New concepts are based on variable speed with pitch control and either direct driven synchronous ring generator or doubly-fed asynchronous generator [32].

In this licentiate report a model is used to obtain the power output from a wind turbine using the wind speed as input. This is achieved by using the so-called wind-power curve of a wind turbine. The wind-power curve is the relation between the wind speed and the power output of the wind turbine and differs for different types of wind turbines.

The wind-power curve used for this model is valid for a 1000 kW stall regulated wind turbine. The curve can be seen in figure 3.25. The data has been normalized to be more general. It is normalized to 1 kW at nominal power (P_n). The data holds for a state-of-the-art commercial wind turbine [22].

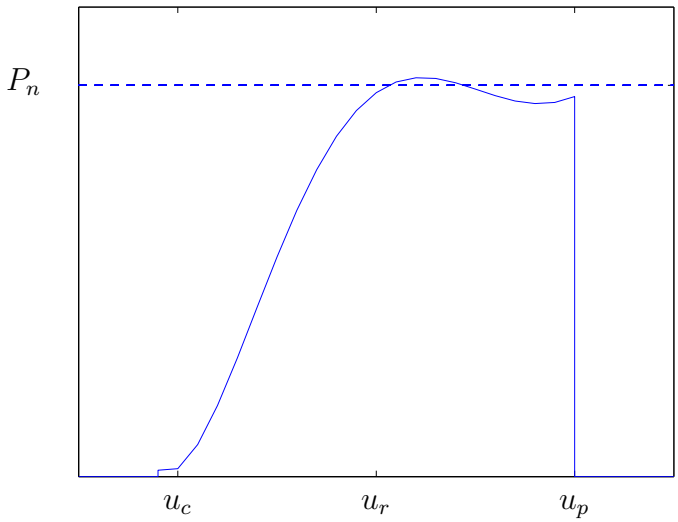

Figure 3.25: Model wind turbine power output versus wind speed.

The curve is defined mathematically by equation 3.16.

$$P = \begin{cases} 0, & v < u_c \\ Av^5 + Bv^4 + Cv^3 + Dv^2 + Ev + F, & u_c \leq v \leq u_p \\ 0, & v > u_p \end{cases} \tag{3.16}$$

The coefficients in equation 3.16 are: A$=-2.0763 \cdot 10^{-6}$, B$=2.0046 \cdot 10^{-4}$, C$=-7.0343 \cdot 10^{-3}$, D$=0.1067$, E$=-0.5965$ and F$=1.0963$.

The cut-in wind speed (u_c) is normally set to 4 m/s and is the minimal wind speed needed for the wind turbine to generate power. If the wind speed is less then u_c there is not enough power in the wind to cover the friction and other losses in the wind turbine. The wind speed for nominal power output is u_r and is a design parameter, normally 15 m/s. If the wind speed exceeds a certain value (u_p) the wind turbine has to be shut down to protect the turbine. The protection wind speed is normally 25 m/s.

3.4 Load model

In reliability calculations the loads are a important factor since it sets the demands. The load determines what should be achieved. The load curve in this thesis can be seen in figure 3.26. The load curve was selected to represent both daytime load (industry mainly) and lower night time load (education and leisure activities). The level of the load has been set to a daily average value of 15 kW which corresponds to an energy consumption of 360 kWh/day.

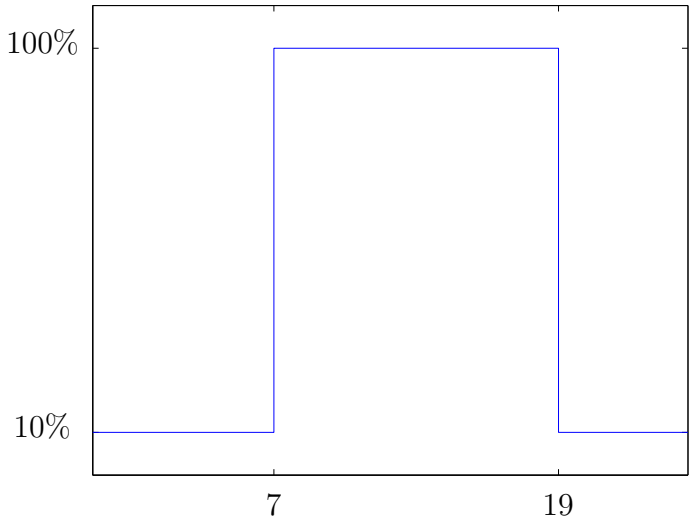

Figure 3.26: The shape of the load used for the reliability calculations.

In industrial countries the load curve is a combination of domestic, industrial and commercial loads. Both systems and load are more or less fixed. In the kind of remote networks that are a subject of this licentiate report, the load situation is a completely different one. In the existing situation there is no or little electrical load. The load curve is therefore much more uncertain but also more adaptable than in industrial countries. Industry activities can be planned after the access of power. Since one of the generation sources is sun, the high loads are desired during hours with sun (daytime).

Since the main purpose of this study is to rise the living standard in development countries there is a need to create an environment of generating income to the area, like starting and make profit from companies. The size of the companies will probably be small initially but with potential to grow if the right people are involved. One way of getting the most out of the system and sharing its resources is to use local controlled load sharing.

There are many ways of sharing load but if the power is so restricted as it in this case a possible sharing technique would be sharing days when one company is allowed to use the whole system and the others have strong restrictions and then the next day it is the other way around. Of course there will be problems since the conditions could change for one day to another and therefore local control is a necessity.

3.5 Storage model

There are today many different methods of storing energy, mechanical (PHES, CAES, FES), electrical(SMES, ACAP) and electrochemical (BESS, FB, Fuel cells) [33]. Which one that is the most advantages are dependent on the size of the storage capability, geographical location and control strategies.

Many comparisons have been made and according to [34, 35] the there are two different

interesting cases of storage, load levelling (long term) and power quality (short term). The long term are often close connected to large storage while short term is strongly connected to a small storage capability which should only inject power if necessary. Methods of storage that are suitable for short term storage are BESS, SMES, ACAP and FES while for long term are BESS, CAES and PHES more suitable. Fuel cells or flow battery are also for long term storage since it require some startup time [34] and the storage capability are almost only depend on the size of the storage tanks. The start time occurs because of the need of the chemical reaction to be reversed.

Here follows a short presentation of the today existing storage technologies.

Flow Batteries or regenerative fuels cells (FB)

In a storage system of flow batteries is energy stored as chemical potential energy. The chemical potential energy will be created by "charging" the two liquid electrolyte when they are pumped through a cell which has two electrodes and a proton exchange membrane when a potential is applied between the electrodes. The energy will be released when the procedure is reversed with a a load connected between the electrodes. There are many different couples of electrolytes and an example that is today commercialized is polysulphide/bromide and in equation 3.17 is the simplified overall chemical reaction, for this combination of fuel cells, is shown.

$$3NaBr + Na_2S_4 \Leftrightarrow 2Na_2S_2 + NaBr_3 \tag{3.17}$$

The main advantage of flow batteries are that the are useful for utility-scale energy storage if combined with large storage of electrolyte. One of the disadvantages are the hazards of using and working with chemicals that are not environmental friendly [33]. Today are the appears the focus be mainly in the automotive industry, like buses/trucks which can be seen as isolated power system.

Super conducting Magnetic Energy Storage (SMES)

A super conducting magnetic energy storage is based on storage of energy in a magnetic field of a super conducting coil. To obtain the super conducting state of the coil it must be held at cryogenic temperature. This requires a refrigerating system with use of liquid helium or nitrogen [36, 37]. The super conducting coil can be configured as solenoid or a toroid. The solenoid is the most common due to its simplicity and cost effectiveness but the toroid-shape has been used in a number of small SMES systems [36]. Energy can be stored for several month in a SMES system but it has still the access time is still just a few milliseconds. SMES has low maintenance due to no moving parts and its life time is independent of number of charges/discharges [37]. Compared with other energy storage technologies SMES is still to costly be alternative but previous studies have shown that micro (< 0.1 MWh) and midsize (1-100 MWh) has a great potential in the future on transmission and distribution levels. Use of high temperature super conductors would also improve the cost effectiveness of the SMES in the future [36]. SMES has been used in a number of installations to mitigate power quality disturbances [38].

Battery Energy Storage Systems (BESS)

Batteries are perhaps the most cost effective electrochemical energy storage. There are today many types of batteries, lead-acid, nickel-cadmium, hydride batteries, nickel-metal and lithium-ion etc., and the most used today is lead-acid [36] but nickel-cadmium is believed to be something for the future due to higher charge density and lower lifetime cost [34]. The lead-acid battery is today an mature technology and used for bulk energy storage and for rapid charge/discharge. A main disadvantages are the low cycle life, low energy density and environmental hazard during the entire life time of the battery. The main advantages are low installation cost and possibilities for sealed battery, which is necessary for mobil applications [36]. The benefits from nickel-cadmium batteries are long life time, high reliability, low maintenance, low cycle cost and environmental friendly [34]. Batteries are today a well used storage technology are are almost used everywhere.

Advanced Capacitors (ACAP)

An advanced capacitor stores energy in a electric field by accumulating a positive and negative charges on two plates separated by an insulating dielectric. The energy E that can be stored in a capacitor can described by equation 3.18 where ϵ is the permittivity of the dielectric, A is the area of the plates, d is the distance between the plates and V is the voltage between the plates.

$$E = \frac{1}{2}\frac{\epsilon A}{d} \cdot V^2 \tag{3.18}$$

Capacitors have today a limited use as large-scale energy storage device for power systems and are today only used for short-term storage in power converters. In the future ceramic hyper capacitors and super capacitors (Ultra Capacitors) could be useable as large-scale storage in power systems. Ceramic hyper capacitors have a high withstand voltage and a high dielectric strength but the are not good enough today to be useful. In cryogenic operation they appears to be more interesting but that is perhaps something for the future. Super capacitors are double layers capacitors and thereby have an increase in storage capability. Super capacitors are most useful for high peak-load, low energy situations [36]. The number of charging/discharing cycles are above 10^6 for a ACAP and there is no decrease in storage capacity for increasing number of cycles [37]. ACAP is often used as very short-term storage in power converters and in small mobile telecommunication devices (GSM) [36].

Flywheel Energy Storage (FES)

The methods of storing energy in Flywheel is based on the accelerating and retardation of a rotating mass. The energy stored in the flywheel can be described by equation 3.19 where E is the energy, r is the radius of the mass, m is the weight of the mass, l is the length of the mass and ω is the rotation velocity of the wheel.

$$E = \frac{r^2 m l \omega^2}{4} \tag{3.19}$$

There are two different strategies when constructing a flywheel, high (approx. 100 000 rpm) and low (approx. 10 000 rpm) rotation velocity [36]. A flywheel with the low rotation velocity has a large mass, often steel, with a large radius while the high rotation velocity has a smaller mass often of resin/glass or resin/carbon-fiber [39]. Another important difference between the different rotation velocities are the demands on the motor/generator. For a flywheel with high rotation velocity a needed very high speed motor/generater is needed while a low rotation velocity flywheel can use a fairly standard motor/generator [36].

There are several advantages with the flywheel method. The method is capable of up to 100 000 charge/discharge cycles and is in practice independent of temperature. The methods as also a low impact on the environment since there are no emissions during the life except for the manufacturing and disposal of the parts of the flywheel [40].

Today the flywheels have limitation to be used for long-term storage but are useful for use in uninterruptible power supplies (UPS). To be able to use flywheel as long-term storage the losses needs to be reduced. A solution to the problem might be super conducting magnetic bearings and vacuum vessels for the mass. FES has similar applications areas as SMES and in transportation [36].

Pumped Hydro Electric Systems (PHES)

Storing energy by increasing the potential energy in water is a mature technology that are today used at several hundred locations. The "stored" energy can be easily be converted to electric energy by releasing the water to drop from a higher reservoir to an lower reservoir through hydro turbines. The energy stored in upper reservoir can be described by equation 3.20 where E is the energy, ρ is the density of water, V is the volume of water, g is the acceleration of gravity and h is the height between the turbine and the mean water level in the upper reservoir.

$$E = \rho V g h \tag{3.20}$$

The generation and pumping can either the be accomplished by a single-unit, reversible pump-turbine or by separate pump and turbine. Mode changes for the systems can occur in a time period of minutes. One of the major problems with this technology is ecological, two water reservoirs are needed and not far from the consumers. There are today at least 285 active pumping power plants world wide [37], so this is a today technology mature for use in power systems

Compressed Air Energy Storage (CAES)

CAES is based on a method that compresses air into some kind of storage during low load hours and then by the use of an conventional natural gas combustor to recover the electric energy during high load hours. There are two different types of storages for CEAS systems, under ground and vessels. The under ground systems could have storage in naturally occurring aquifers, old salt caverns and mechanically formed reservoirs in rock formations. Storage systems with vessels (also called CAS) are normally a more expensive solution but not dependent on the location [35].

Comparison for different storage methods

The various methods described in the sections above have different efficiencies. In table 3.5 an overview of the different storage methods is shown.

Table 3.5: An overview of different storage methods.

Storage Method	Eff[a] [%]	Number of charge cycles	Allowed max. Discharge [%]	Size	Ref.
Fuel cells		c	100	<120 MWh	[41]
SMES	90+refrig.	c	100	50-3000 MJ	[42, 43]
BESS	$80-85$	3000[b]	80	<144 GJ	[37, 34, 38]
ACAP	95	10^6	100	<1 MJ	[37, 35]
FES	$90-95$	10^5	80	<5 MJ	[37, 40, 36]
PHES	$75-80$	c	100	d	[37]
CAES	70	c	100	d	[35]

[a] : Efficiency.
[b] : at discharge rate of 80%.
c : dependent of lifetime of the physical components.
d : dependent of size of reservoir.

Which one to use is dependent on various factors like geographical conditions but some may be ruled out directly, ACAP and FES. ACAP and FES have today too small capacities. The economical aspect is of course also important.

3.5.1 Model used in this thesis

No one knows what the future will be showing in this research area and that is why ideal storage has been used. An ideal storage device is a device with 100% efficiency and it can be discharged/charged at any level and to 0/100% if needed.

Chapter 4

Case Study, Timbuktu

In this part of the thesis, the models presented in the previous chapter are used for a number of case studies. All below listed combinations regarding the models are both presented individually and discussed. Twelve different cases were investigated:

- Solar power only
- Solar power with ideal storage
- Solar and hydro power
- Solar and hydro power with ideal storage
- Wind power only
- Wind power with ideal storage
- Solar and wind power
- Solar and wind power with ideal storage
- Wind and hydro power
- Wind and hydro power with ideal storage
- Solar, wind and hydro power
- Solar, wind and hydro power with ideal storage

Cases with only hydro or hydro with ideal storage are not considered. The hydro power model is constant and therefor gives no stochastic behavior.

In this chapter the following nomenclature is used:

P_{sun}	Power generated by solar radiation
P_{wind}	Power generated by wind
P_{water}	Power generated by flow-of-river (hydro)
P_{load}	Load of the system
MGC_{solar}	Maximum Generation Capacity for solar power generation
MGC_{wind}	Maximum Generation Capacity for wind power generation
ϵ_{stor}	The energy in the ideal storage
$\epsilon_{stor}(i)$	The energy in the ideal storage at current step in simulation
$\epsilon_{stor}(i+1)$	The energy in the ideal storage at the following step in the simulation
ϵ_{stor}^{max}	The maximum energy that could be stored in the ideal storage
$\Delta\epsilon_{stor}$	The change of energy in the ideal storage
ϵ_{water}	The energy in the reservoir
$\epsilon_{water}(i)$	The energy in the reservoir at current step in simulation
$\epsilon_{water}(i+1)$	The energy in the reservoir at the following step in the simulation
ϵ_{water}^{max}	The maximum energy that could be stored in the reservoir
$\Delta\epsilon_{water}$	The change of energy in the reservoir

The solar model requires a geographical location. For this study the location of Timbuktu has been chosen, which is the capital of Mali in the southwest of Africa. Timbuktu is located at a Latitude 16.75 °N and Longitude of 3.07 °W and the local time is equal to the GMT. Timbuktu is chosen due to its location and the fact that Mali is a developming country with typical African/Sahara climate according to Köppen´s climate classification system [15]. Figure 4.1 shows a map over Africa and Mali.

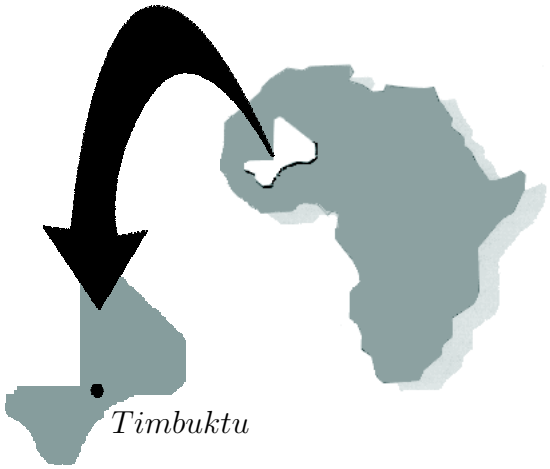

Figure 4.1: A map over Africa showing Mali and Timbuktu.

Assumptions that has been made except those presented in the models are no losses and no faults on the power system components. The control of the power system are assumed to be done by ideal power electronics. Meteorological data, used as input for models, are due to lack of data from Timbuktu, measured in Sweden. Cloud coverage data were collected at Säve Airport, Göteborg and wind speed data were collected at Näsudden, Gotland and at Säve Airport, Göteborg.

To be able to relate the generation capacity used in the simulation to the load and to compare different power sources the Maximum Generation Capacity (MGC) is used. The MGC_{solar} is the ratio between the theoretical maximum power generation (when the sun is in zenith during a cloudless day) and the maximum load for the solar power generation. MGC_{wind} is calculated as the ratio between the rated wind power and maximum load.

As described in Chapter 2 the basis of Monte-Carlo simulation are repeated simulations. In this case studies only one simulation is performed for each data point because as shown in Figure 4.2 little extra useful information will be achieved by repeating the simulation. In the figure the solid line, showing the mean value of ten simulations, has a very resemblance with the dashed line, that shows the result of only one simulation. By using only one simulation per data point computational time will be significantly reduced.

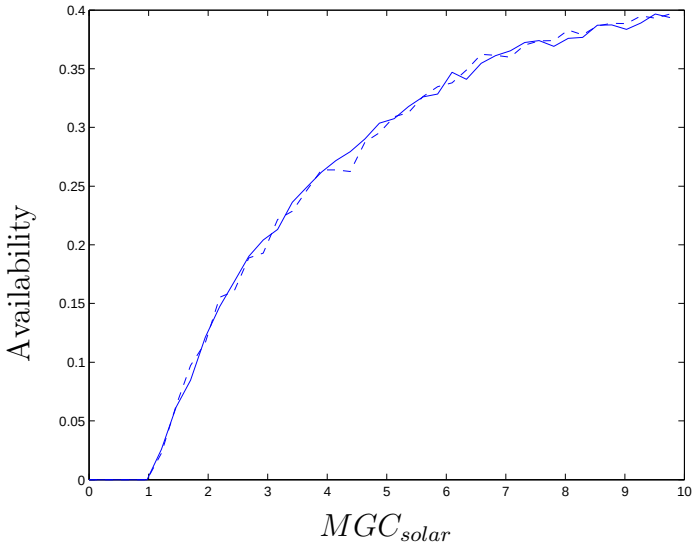

Figure 4.2: Availability of a power system with only solar power generation where the solid line indicates the mean value of ten simulations while the dashed line is the result from a single simulation.

For the reliability calculations in this chapter a time step of one hour is used despite the stochastic varying models, presented in previous chapter, being developed for shorter time steps. From Figure 4.3 and 4.4 it can be concluded that the there is little need of smaller time steps then one hour in this kinds of calculations. Figure 4.3 shows the the case of only solar power and load and Figure 4.4 shows a system where the power generation originates from wind power. The differences seen in the figures are not greater then the difference between two different simulations. A difference should not occur because the mean value is independent on the length of the time steps. In some cases the use of smaller time step is a necessity, like calculations of number of times shortage occurs and the duration of the shortages. This kinds of calculations are anyway done in this thesis with a time step one hour. These studies are just an estimation of different system configurations and to be able to compare different configurations and therefor shorter times are at this stage not necessary. Especially when using storage or hydro, the short-term fluctuations in solar and wind will be smoothened out.

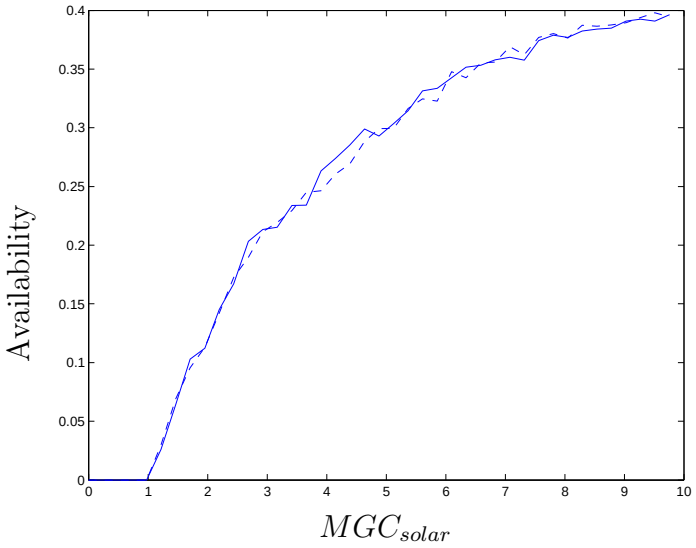

Figure 4.3: A comparison between availability calculation with different time steps, one hour (solid line) and 6 minutes (dashed line).

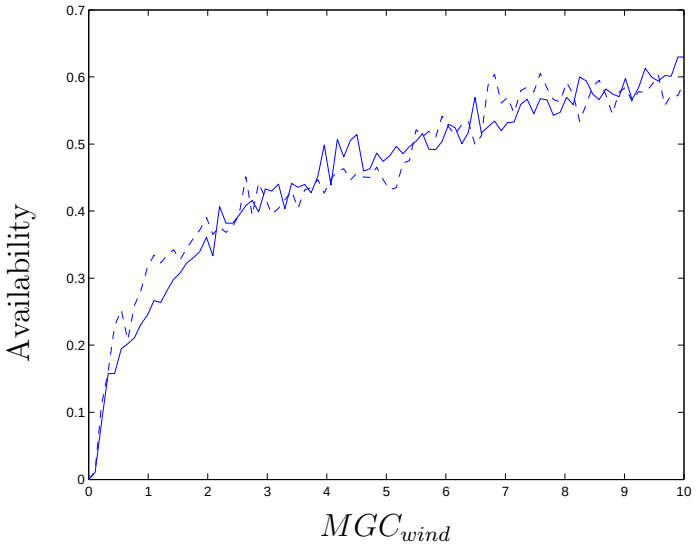

Figure 4.4: A comparison between availability calculation with different time steps, one hour (solid line) and 10 minutes (dashed line).

4.1 Solar power only

The most simple power system and the first case in this study is a power system with only solar power as power source and no storage. In Figure 4.5 this system is schematically shown. The supplying energy and load are calculated according to earlier explained models and the load is considered supplied if:

$$P_{sun} \geq P_{load} \tag{4.1}$$

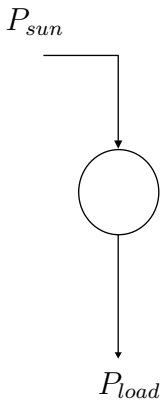

Figure 4.5: Model of power flow in a small power system with only solar power as power source.

Figure 4.6 shows the availability as function of MGC_{solar}. For large generation capacity the availability nears 50 % but it never exceeds this level because the sun is above the horizon for only 50% of the time. We also see that a large overcapacity is needed to obtain a reasonable availability. For a 40% availability (80% of day time), the installed capacity should be about 10 times the maximum load. Figure 4.7 shows the load and the power supply during a few days. It clearly indicates the lack of solar during nighttime. But not only during night time does this lack of power exist. In dawn and in dusk there are also some problems because beginning and end of the power production is dependent of the season since dawn and dusk change over the year and the load, is assumed season-independent. The great 24 hours period dependence is maybe the largest disadvantage of solar power generation. However, as we will see later in combination with some other power sources solar power generation can be used.

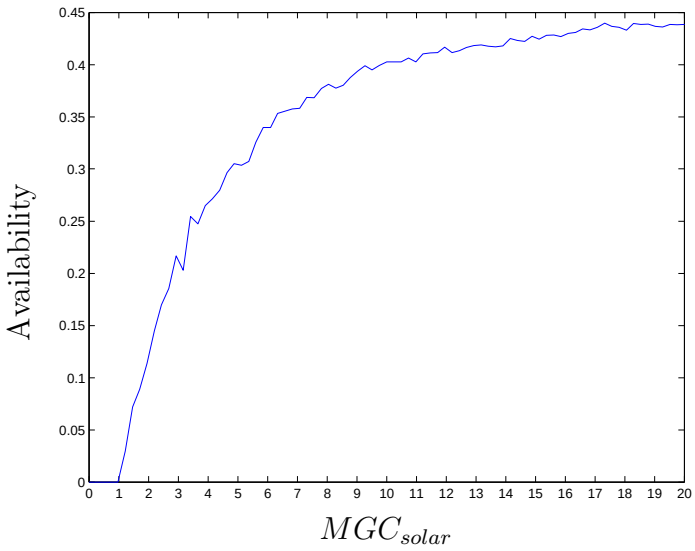

Figure 4.6: The availability of a system with only solar power.

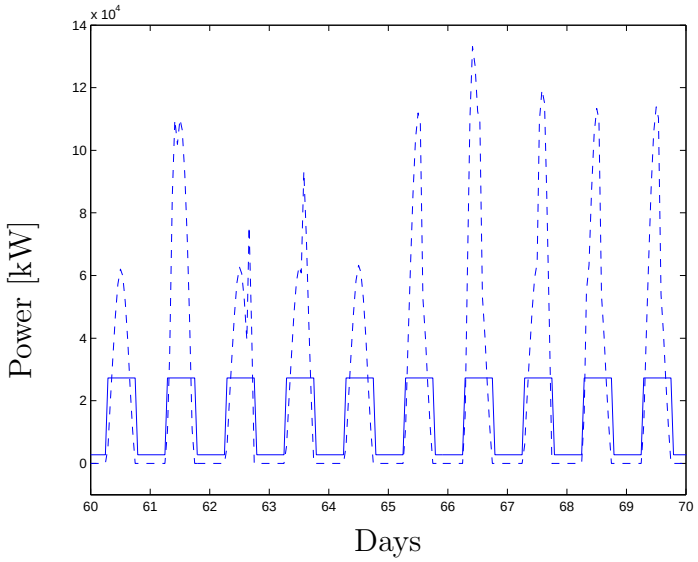

Figure 4.7: A comparison between load (solid line) and available power (dashed line).

4.2 Solar power with ideal storage

By combining the solar power generation with storage the most obvious problems with solar power can be avoided. As can be seen in Figure 4.7 the solar capacity often exceeds the load. But at other times the solar capacity is insufficient. By storing the daytime surplus and use it at night, the availability will be improved. In Figure 4.8 a model of the system is shown. The system uses solar power; the surplus of power is stored and then used when needed. The load is considered supplied if:

$$P_{sun} + \epsilon_{stor}(i) \geq P_{load} \tag{4.2}$$

The change in storage is calculated as follows:

$$\Delta\epsilon_{stor} = P_{load} - P_{sun} \tag{4.3}$$

$$\epsilon_{stor}(i+1) = \begin{cases} \epsilon_{stor}(i) + \Delta\epsilon_{stor} & \Delta\epsilon_{stor} < \epsilon_{stor}(i) \\ 0 & \Delta\epsilon_{stor} \geq \epsilon_{stor}(i) \end{cases} \tag{4.4}$$

unless $\epsilon_{stor}(i+1)$ exceeds ϵ_{stor}^{max} then

$$\epsilon_{stor}(i+1) = \epsilon_{stor}^{max} \tag{4.5}$$

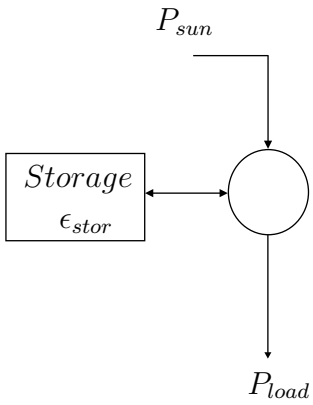

Figure 4.8: Model of power flow in a small power system with use of solar power and ideal storage.

An important factor affecting the availability is the storage capacity (ϵ_{stor}^{max}) and that is why Figure 4.9 shows the availability curve for five different storage capacities. The number next to the lines represents the storage capacity, which is the number times maximum load. The line marked with 0 refers to a none-storage system as in Figure 4.2. From this figure it can be concluded that 90% availability can be obtained with 7 times maximum load of solar panels and 3 times maximum load of storage.

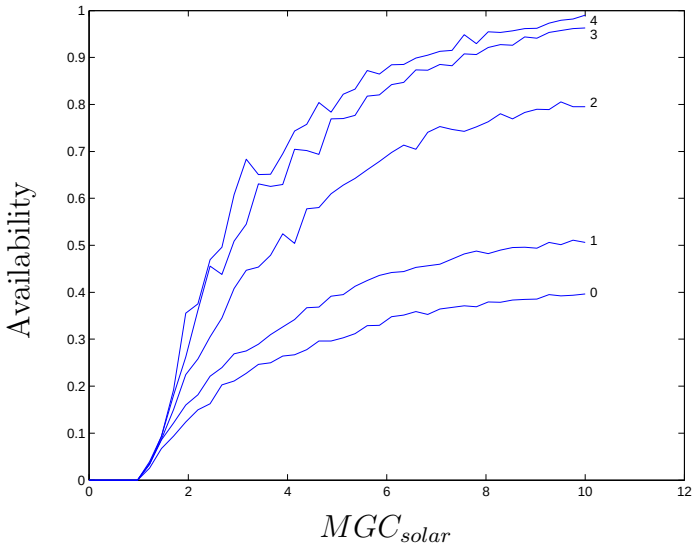

Figure 4.9: A comparison between different maximum storage capacities. 0: none-storage system, 1: storage capacity equal to the maximum load, 2: Storage capacity twice the maximum load, 3: Storage capacity of three times the maximum load and 4: storage capacity of four times the maximum load.

Figure 4.10 shows the energy level in the storage for a few days. A typical trend is noticeable that the storage is filled during daytime and then emptied during nighttime which is expected for a solar power system. In the figure MGC_{solar} is 10.0 and the maximum storage is 3.0 times the maximum load.

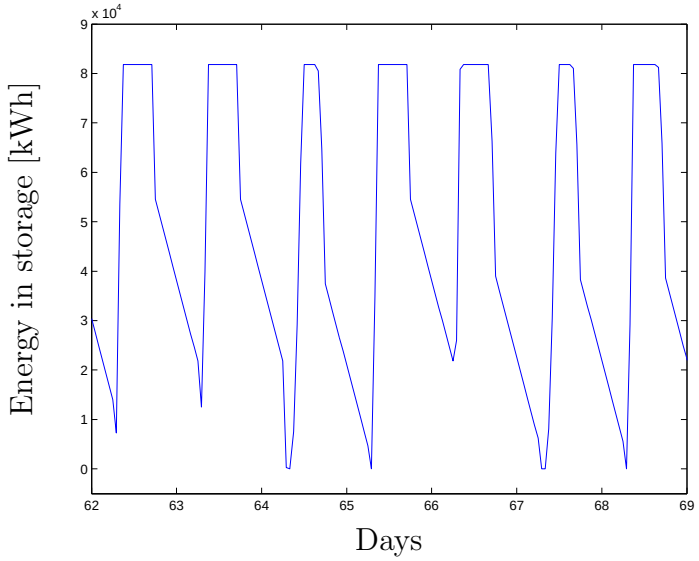

Figure 4.10: The amount of energy in the storage for a few days.

4.3 Solar and hydro power

The largest problem with solar power is to cover the sunless hours during the night. The solution with combining with storage is one way but it requires large storage capacities to achieve reasonable reliability of the system. Another solution to the problem would be to have a constant power source as a complement to the solar power, preferably another renewable source. A flow-of-river could be such a power source. If it is combined with a small reservoir then benefit could be even greater without adding any larger economical investment. In Figure 4.11 a model of such system is shown. The availability as a function of MGC_{solar} is shown in Figure 4.12 and the flow-of-river is 0.1 times maximum load and the reservoir size corresponds to 1.0 hour of maximum load. The load is considered supplied if:

$$P_{sun} + \epsilon_{water}(i) \geq P_{load} \tag{4.6}$$

and energy in the reservoir could be calculated as follows:

$$\Delta\epsilon_{water} = P_{load} - P_{sun} \tag{4.7}$$

$$\epsilon_{water}(i+1) = \begin{cases} \epsilon_{water}(i) + P_{water} & \Delta\epsilon_{water} \leq 0 \\ \epsilon_{water}(i) + P_{water} - \Delta\epsilon_{water} & 0 < \Delta\epsilon_{water} < \epsilon_{water}(i) \\ P_{water} & \Delta\epsilon_{water} \geq \epsilon_{water}(i) \end{cases} \tag{4.8}$$

unless $\epsilon_{water}(i+1)$ exceeds ϵ_{water}^{max} because then should

$$\epsilon_{water}(i+1) = \epsilon_{water}^{max} \tag{4.9}$$

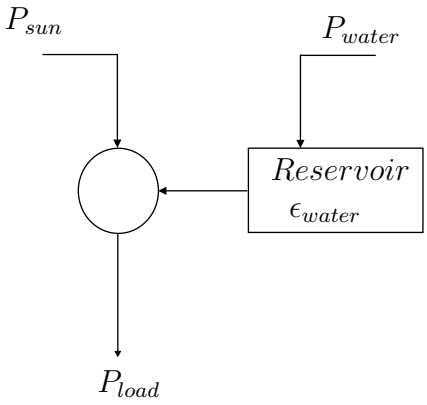

Figure 4.11: Model of power flow in a small power system with use of solar and hydro power.

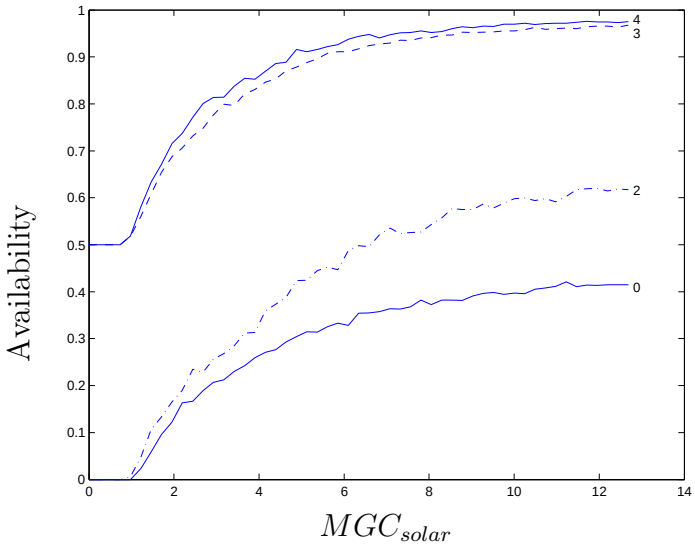

Figure 4.12: The availability of a system that combines solar energy, flow-of-river and a small reservoir. The numbers in the figure represents: 0: No part of hydro power used, 2: The power of hydro corresponds to 7 % of maximum load, 3: The power of hydro corresponds to 10 % of maximum load, 4: The power of hydro corresponds to 13 % of maximum load.

As seen in Figure 4.12 the difference of using a flow-of-river of 10 % instead of 7 % corresponding to maximum load is greater, due to the 10 % supplies the load to 100% during low load hours (night time). By increasing the hydro power part even further, is no use if the increase is not significantly so that the hydro power will be a significantly part of maximum load.

The benefit of using a simple reservoir can be seen in Figure 4.13. The solid line shows the availability as a function of capacity of the reservoir while the dashed line shows the case without reservoir. The gain of using a reservoir is larger the greater the reservoir. The calculation without reservoir is of course independent of the reservoir size. The fluctuation in the dashed curve are due to the random variations inherent to the Monte-Carlo simulation.

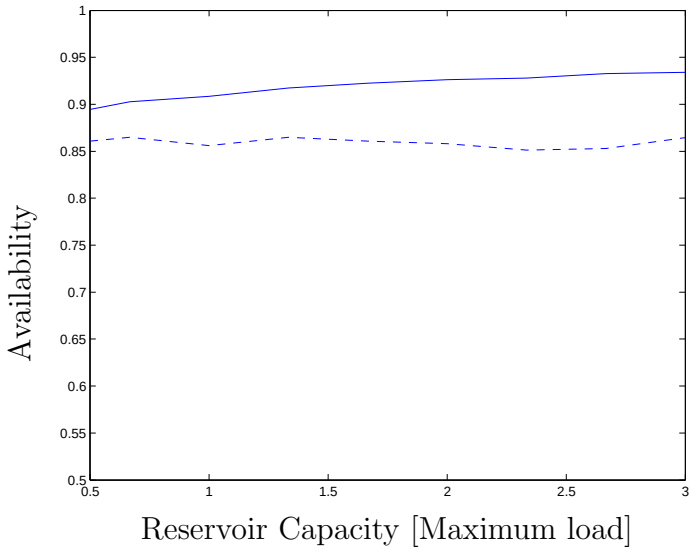

Figure 4.13: A comparison for power system with (solid) and without (dashed) reservoir.

4.4 Solar and hydro power with ideal storage

By adding the hydro power to the solar power generation the availability increased significantly mainly during nighttime. By combining the system with storage capacity could increase the availability of the system even further. A model of such a system is shown in Figure 4.14 and the availability is calculated according to the equations below. The load was considered supplied if:

$$P_{sun} + \epsilon_{stor}(i) + \epsilon_{water}(i) \geq P_{load} \tag{4.10}$$

and the energy in the storages will then be:

$$\Delta\epsilon_{stor} = P_{load} - P_{sun} \tag{4.11}$$

$$\Delta\epsilon_{water} = P_{load} - P_{sun} - \epsilon_{stor}(i) \tag{4.12}$$

$$\epsilon_{stor}(i+1) = \begin{cases} \epsilon_{stor}(i) - \Delta\epsilon_{stor} & \Delta\epsilon_{stor} < \epsilon_{stor}(i) \\ 0 & \Delta\epsilon_{stor} \geq \epsilon_{stor}(i) \end{cases} \tag{4.13}$$

$$\epsilon_{water}(i+1) = \begin{cases} \epsilon_{water}(i) + P_{water} & \Delta\epsilon_{water} \leq 0 \\ \epsilon_{water}(i) + P_{water} - \Delta\epsilon_{water} & 0 < \Delta\epsilon_{water} < \epsilon_{water}(i) \\ P_{water} & \Delta\epsilon_{water} \geq \epsilon_{water}(i) \end{cases} \tag{4.14}$$

if ϵ_{stor} and ϵ_{water} exceed ϵ_{stor}^{max} and ϵ_{water}^{max}, respectively then

$$\epsilon_{stor}(i+1) = \epsilon_{stor}^{max} \quad \text{and} \quad \epsilon_{water}(i+1) = \epsilon_{water}^{max} \tag{4.15}$$

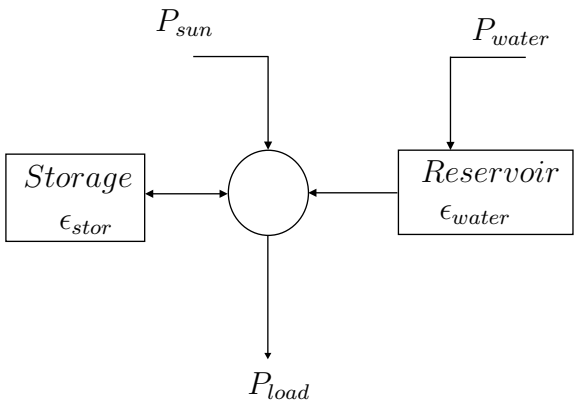

Figure 4.14: Model of power flow in a small power system with use of solar and hydro power in combination with ideal storage.

In the Figure 4.15 the availability of the system is shown. The solid line shows the availability with a none storage system while the dashed-dotted and the dashed line show the availability with storage capacity corresponding to one and three hour of maximum load, respectively. With this configuration it is possible to reach availability approaching 100%. The gain of adding storage appears small but even a gain like a few percentage could be valuable, especially for availability above 90%. In Table 4.1 the number and the length of the shortages are shown for different levels of MGC_{solar}. The flow-of-river is constant at 0.1 of maximum load; reservoir and storage capacity correspond to 1.0 hour of maximum load each. The number of shortages in the table is the mean value of 25 independently simulations.

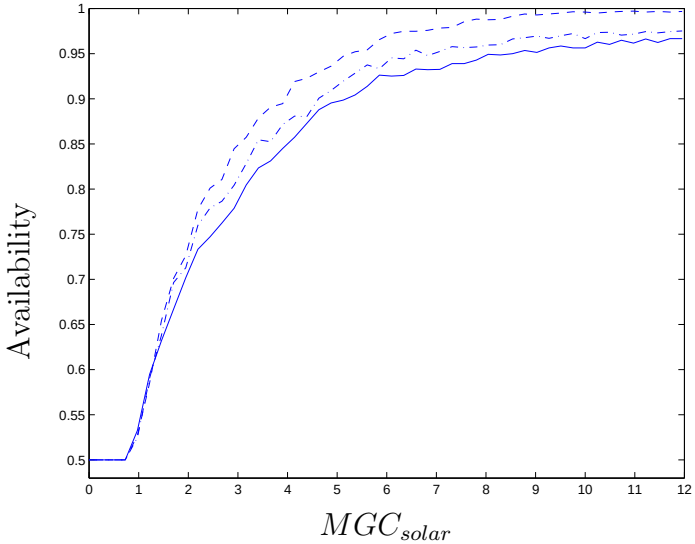

Figure 4.15: The availability of a system with with a combination of solar and hydro power sources and ideal storage. The solid line shows the availability of a system with no storage capability The dashed-dotted and the dashed lines are with a storage capability corresponding to one and three hours of maximum load, respectively.

Table 4.1: Number of shortages for different duration for different MGC_{solar}

Duration [h]	MGC_{solar}				
	1	2	5	10	20
1	10.8	114	176.6	154.3	120.2
2	0	145	80.2	53.8	
3	29.4	8.3	58.1		
4	84.4	80.4	39.7		
5	57.2	22.7	9.6		
6	25.8	16.8			
7	6	1.6			
8	0	0			
9	0	0			
10	0	0			
11	0	0			
12	265.9	96.6			
Total shortages	474.9	567.9	364.1	208.1	120.2
Total hours	4111.8	2135.2	718.1	261.9	120.2
Average h/short.	8.7	3.8	2.0	1.3	1.0

When the load is not supplied that just means that the load is not fully supplied. Figure 4.16 shows the power available for none-fully supplied hours with a MGC_{solar} of 10.0. This power could still be used if some actions were taken to reduce the load. From this calculation it can be seen that for almost 10% of the none supplied hours the are less then 10% power is missing. Thus with a limited load reduction the availability of the rest of the load could be increased.

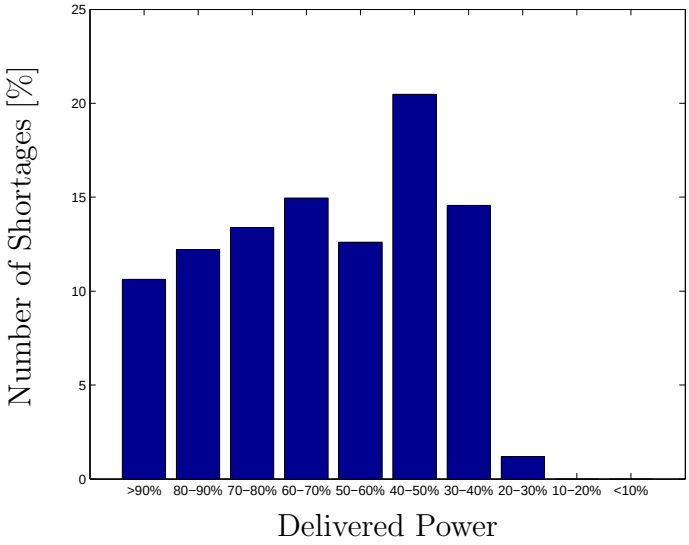

Figure 4.16: The supplied power when the load was not supplied to 100%.

Another important aspect are the time of the day when the shortage occurs. In Figure 4.17 the number of shortages are shown for each hour of the day. The power supply was 5.0 MGC_{solar} and the power from flow-of-river corresponds to 0.1 times maximum load. The storage is 1.0 times maximum load for the storage as well as for the reservoir.

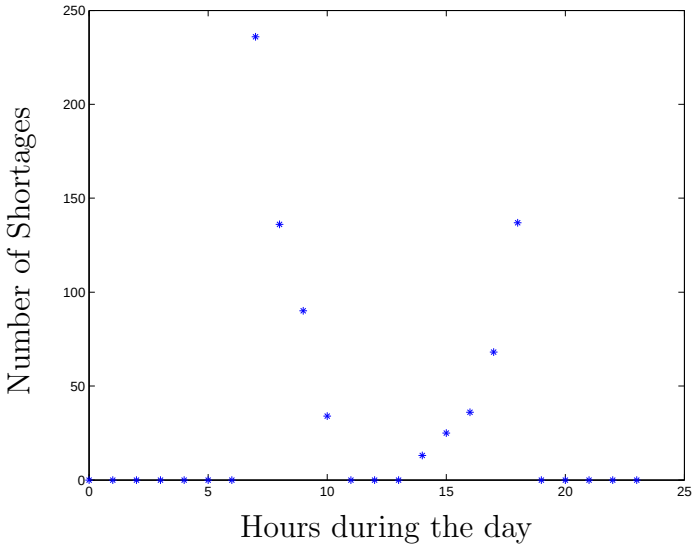

Figure 4.17: Number of shortages for each hour of the day.

The most frequent none-supplied hours are in the morning before dawn and in the evening after dusk, when the load is at maximum. The fact that the problem is more severe in the morning then in the evenings is because of the ideal storage, that were stored during daytime and then used during the evening times and only not used during the evening the stored energy will saved for the morning. The hydro power will cover the night time hours completely.

4.5 Wind power

The sun is not the only available power source. In this case an investigation of wind as power source is conducted. The height of the nacelle is constant at 60 m and will be so for the rest of the calculation that includes wind power. In Figure 4.18 a model to calculate the reliability of such system is shown. The load will be considered supplied if:

$$P_{wind} \geq P_{load} \tag{4.16}$$

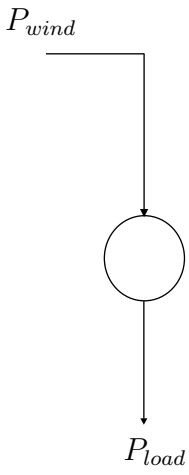

Figure 4.18: Model of power flow in a small power system with use of wind power.

Figure 4.19 shows the availability for the system shown i Figure 4.18. Availability is calculated for different values of MGC_{wind}. Again a large overcapacity is needed to obtain an availability more than a few tens of percent. Availabilities more then 65% are hard to obtain with only wind power. Note that the fast fluctuations in Figure 4.19 are "stochastic noise" inherent to the Monte-Carlo simulation.

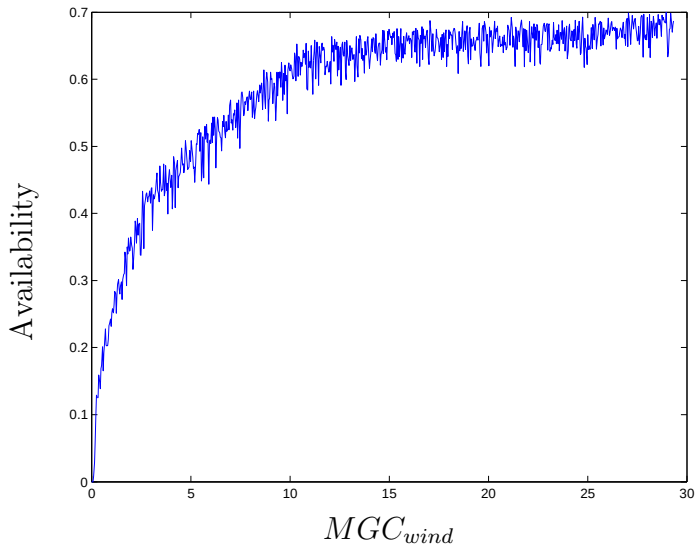

Figure 4.19: The availability of a system with only wind power.

The power supplied from wind power has not a regular (daily) pattern as solar power has. The fluctuations in wind power during a 10-day period can be seen in Figure 4.20. The availability differences between low and high load hours (i.e. between night and day) are small for wind power. The figure is calculated with $MGC_{wind} = 10$.

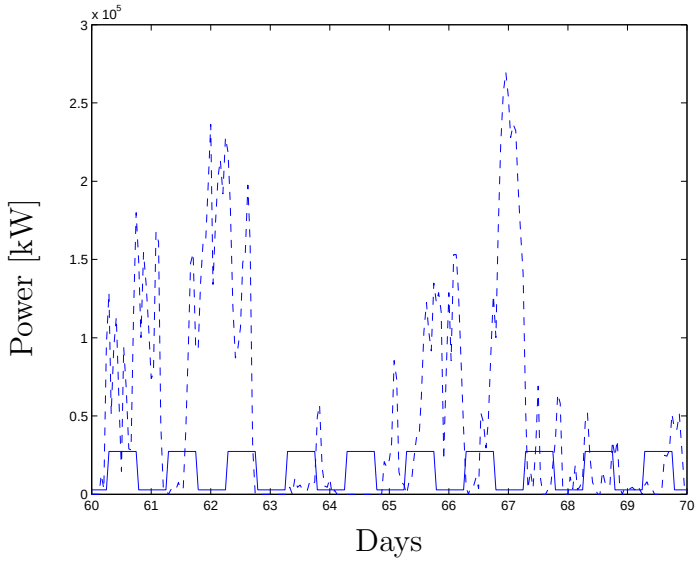

Figure 4.20: A comparison between the power supplied by wind and the load.

4.6 Wind power with ideal storage

The irregularity of the wind power might be avoided by adding some storage capacity. A model of a wind power system with storage is shown in Figure 4.21. The availability

of the system is shown in Figure 4.22. The availability was calculated according to the equations below and the load was considered supplied if:

$$P_{wind} + \epsilon_{stor}(i) \geq P_{load} \tag{4.17}$$

The change in storage is calculated as follows:

$$\Delta\epsilon_{stor} = P_{load} - P_{wind} \tag{4.18}$$

$$\epsilon_{stor}(i+1) = \begin{cases} \epsilon_{stor}(i) + \Delta\epsilon_{stor} & \Delta\epsilon_{stor} < \epsilon_{stor}(i) \\ 0 & \Delta\epsilon_{stor} \geq \epsilon_{stor}(i) \end{cases} \tag{4.19}$$

unless $\epsilon_{stor}(i+1)$ exceeds ϵ_{stor}^{max} then

$$\epsilon_{stor}(i+1) = \epsilon_{stor}^{max} \tag{4.20}$$

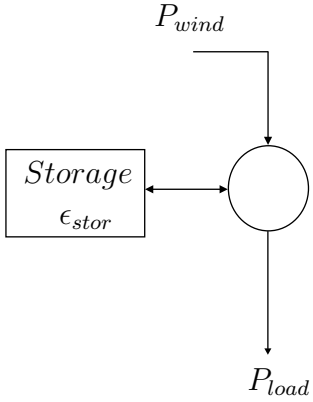

Figure 4.21: Model of power flow in a small power system with wind power and storage.

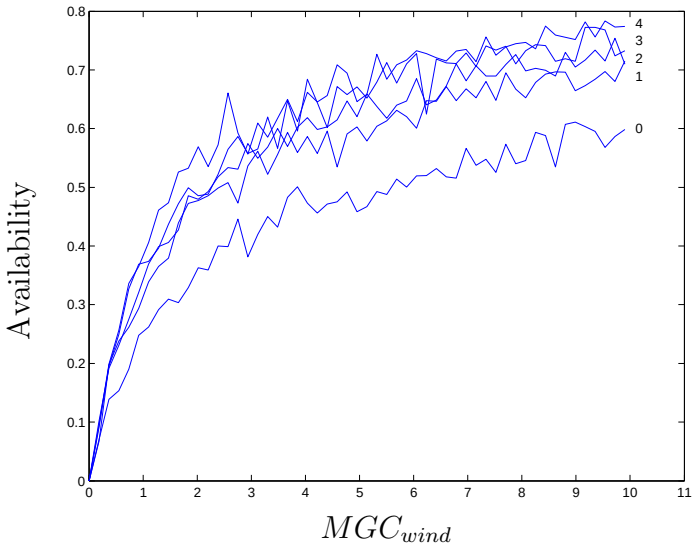

Figure 4.22: A comparison between the power supplied by wind and the load.

In Figure 4.23 the amount of stored energy are shown for a few days. In the calculation the MGC_{wind} and the storage capacity corresponded to 3.0 hours of maximum load.

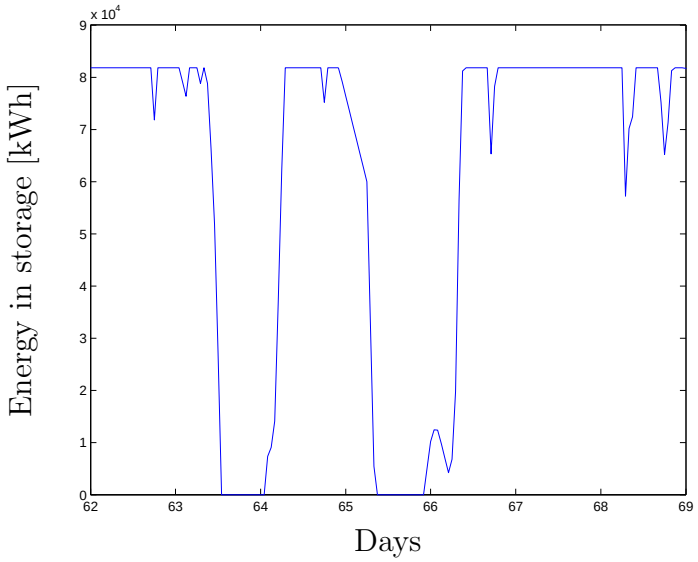

Figure 4.23: The energy level in the storage for a few days.

4.7 Solar and wind power

By using solar and wind power the benefits from both power sources will be combined. A model of such system is shown in Figure 4.24. The availability can calculated as follows. The load is considered supplied if:

$$P_{sun} + P_{wind} \geq P_{load} \tag{4.21}$$

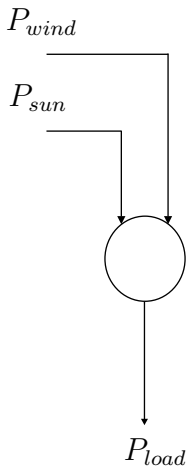

Figure 4.24: Model of power flow in a small power system with use of solar and wind power.

The availability is shown in Figure 4.25 and for different amount of solar and wind power. The numbers in the figure are the value of MGC_{wind} used for the calculation. The increase in availability due to the increase in the MGC_{wind} decreases with higher values of MGC_{wind}. This gives some kinds of limit for the useful amount of wind power. The exact value is probably dependent on the surrounding parameters.

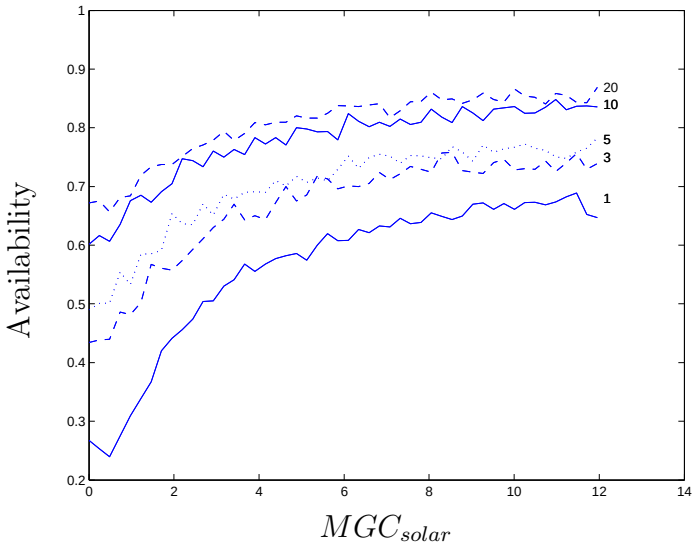

Figure 4.25: The availability for a solar and wind power system. The numbers in the figure represent the value of MGC_{wind} that is used for the calculation.

The non-supplied hours are not equally distributed during the day as can be seen in Figure 4.26. The low number of non-supplied hours during daytime (9 to 16) are because of the during those hours are both solar and wind power available. During other times of the day the solar power is either dependent on the season or not available. To obtain In the figure both MGC_{solar} and MGC_{wind} were set to 5.0.

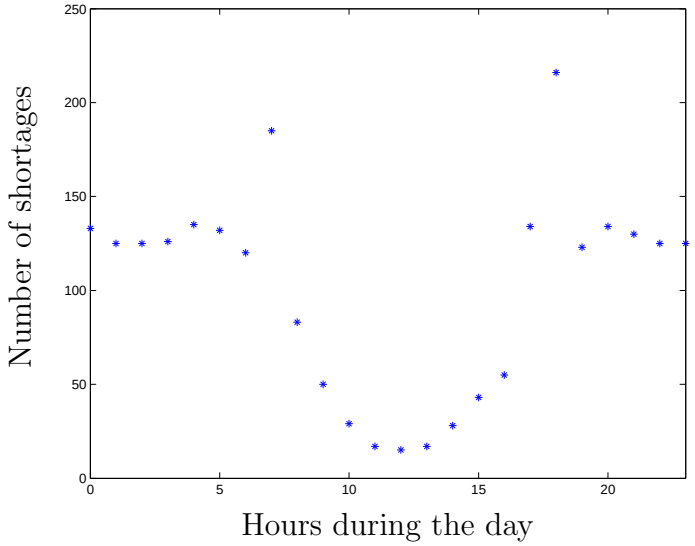

Figure 4.26: The time of the day when the shortages occurs.

4.8 Solar and wind with ideal storage

In the previous section the solar and wind power were combined and in this the eight case was also combined with storage. In Figure 4.27 a model of a solar and wind power system with storage is shown. The availability of the system is calculated as follows and the load is considered supplied if:

$$P_{sun} + P_{wind} + \epsilon_{stor}(i) \geq P_{load} \tag{4.22}$$

The behavior of the storage is ruled by the following expression:

$$\Delta\epsilon_{stor} = P_{load} - P_{sun} - P_{wind} \tag{4.23}$$

$$\epsilon_{stor}(i+1) = \begin{cases} \epsilon_{stor}(i) + \Delta\epsilon_{stor} & \Delta\epsilon_{stor} < \epsilon_{stor}(i) \\ 0 & \Delta\epsilon_{stor} \geq \epsilon_{stor}(i) \end{cases} \tag{4.24}$$

unless $\epsilon_{stor}(i+1)$ exceeds ϵ_{stor}^{max} then

$$\epsilon_{stor}(i+1) = \epsilon_{stor}^{max} \tag{4.25}$$

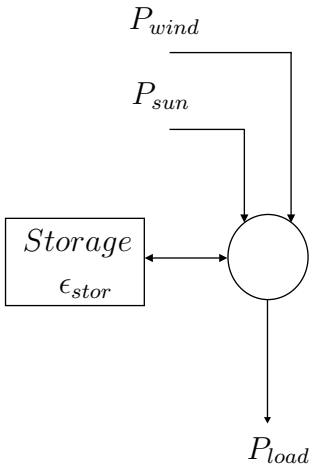

Figure 4.27: Model of power flow in a small power system with use of solar and wind power and ideal storage.

The availability is shown in Figure 4.28 for different storage capacities. For this system it is possible to reach availabilities close to 100%.

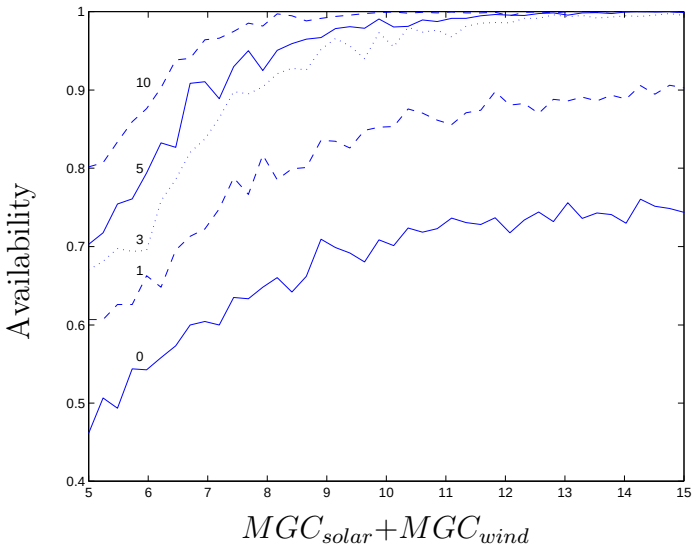

Figure 4.28: The availability for a solar, wind and storage system for different storage capacity. The number represents the capacity of the storage in hours of maximum load and MGC_{wind} is constant at 5.0.

The non-supplied hours for this system are more equable distributed through the day then in the previous case. The main reason for this is the overall much lower number of shortages. In the figure both MGC_{solar} and MGC_{wind} were set to 5.0 and the storage capacity corresponds to three hours of maximum load.

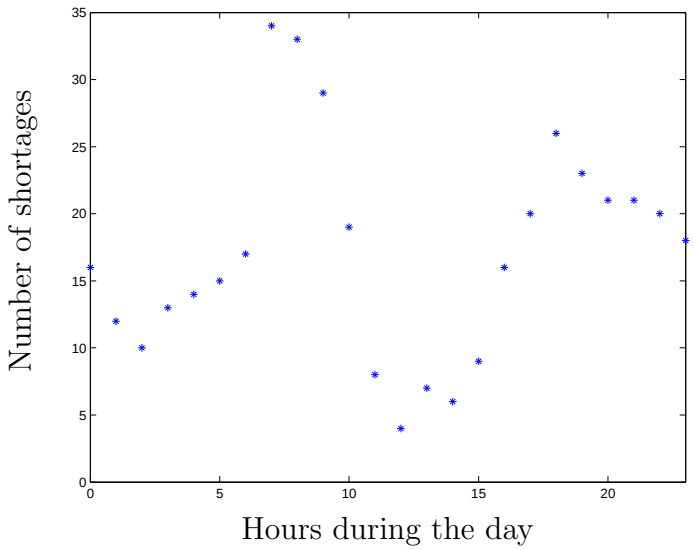

Figure 4.29: The time of the day when the shortages occurs within a solar, wind and storage system.

4.9 Wind and hydro power

In this ninth case a combination of only wind power and hydro power is investigated. A model of a wind and hydro power system is shown in Figure 4.30. The availability for different flow-of-river with a fix reservoir capacity, shown in Figure 4.31, is calculated as shown in the following equations:

$$P_{wind} + \epsilon_{water}(i) \geq P_{load} \tag{4.26}$$

The reservoir behavior is described as:

$$\Delta\epsilon_{water} = P_{load} - P_{wind} \tag{4.27}$$

$$\epsilon_{water}(i+1) = \begin{cases} \epsilon_{water}(i) + P_{water} & \Delta\epsilon_{water} \leq 0 \\ \epsilon_{water}(i) + P_{water} - \Delta\epsilon_{water} & 0 < \Delta\epsilon_{water} < \epsilon_{water}(i) \\ P_{water} & \Delta\epsilon_{water} \geq \epsilon_{water}(i) \end{cases} \tag{4.28}$$

unless $\epsilon_{water}(i+1)$ exceeds ϵ_{water}^{max} because then should:

$$\epsilon_{water}(i+1) = \epsilon_{water}^{max} \tag{4.29}$$

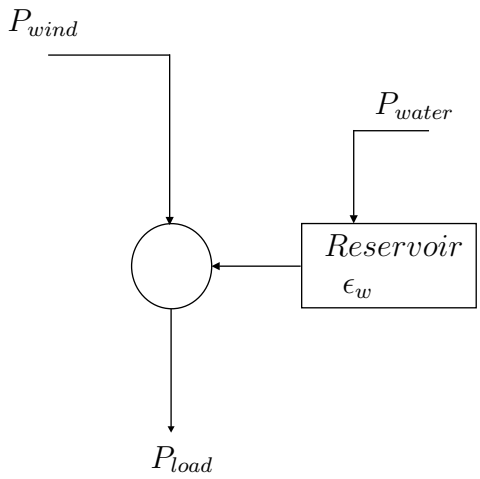

Figure 4.30: Model of power flow in a small power system with use of wind and hydro power.

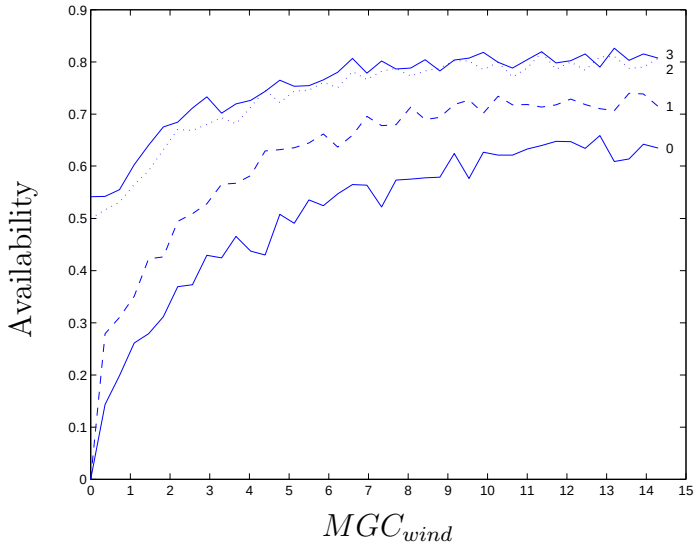

Figure 4.31: The availability of a wind and hydro power systems for different values of available hydro power. 0: No Flow-of-river, 1: The flow-of-river corresponds to 5% of maximum load, 2: The flow-of-river corresponds to 10% of maximum load, 3: The flow-of-river corresponds to 20% of maximum load.

Figure 4.31 shows among others the effect of flow-of-river. The benefit of increasing flow-of-river is small after the 10% limit is reached, because the 10% is enough to supply the system during low load hours (nighttime). The increase in availability for increase flow-of-river above 10% is almost not noticeable, because of the power generation of the flow-of-river is small compared to maximum load. When the flow-of-river increases much more to be a significant part of maximum load, then that will of course make a huge difference in the availability.

4.10 Wind and hydro power with ideal storage

In the previous case the wind and hydro system was investigated. An improvement of the system would be to add storage capacity to the system, a model shown in

Figure 4.32. The availability of wind and hydro system with storage, seen in Figure 4.33, is calculated as in the following equations. The load is considered supplied if:

$$P_{wind} + \epsilon_{stor}(i) + \epsilon_{water}(i) \geq P_{load} \tag{4.30}$$

The behavior of the storage and reservoir is obtained from:

$$\Delta\epsilon_{stor} = P_{load} - P_{wind} \tag{4.31}$$

$$\Delta\epsilon_{water} = P_{load} - P_{wind} - \epsilon_{stor}(i) \tag{4.32}$$

$$\epsilon_{stor}(i+1) = \begin{cases} \epsilon_{stor}(i) - \Delta\epsilon_{stor} & \Delta\epsilon_{stor} < \epsilon_{stor}(i) \\ 0 & \Delta\epsilon_{stor} \geq \epsilon_{stor}(i) \end{cases} \tag{4.33}$$

$$\epsilon_{water}(i+1) = \begin{cases} \epsilon_{water}(i) + P_{water} & \Delta\epsilon_{water} \leq 0 \\ \epsilon_{water}(i) + P_{water} - \Delta\epsilon_{water} & 0 < \Delta\epsilon_{water} < \epsilon_{water}(i) \\ P_{water} & \Delta\epsilon_{water} \geq \epsilon_{water}(i) \end{cases} \tag{4.34}$$

If ϵ_{stor} and ϵ_{water} exceed ϵ_{stor}^{max} and ϵ_{water}^{max}, respectively then

$$\epsilon_{stor}(i+1) = \epsilon_{stor}^{max} \quad \text{and} \quad \epsilon_{water}(i+1) = \epsilon_{water}^{max} \tag{4.35}$$

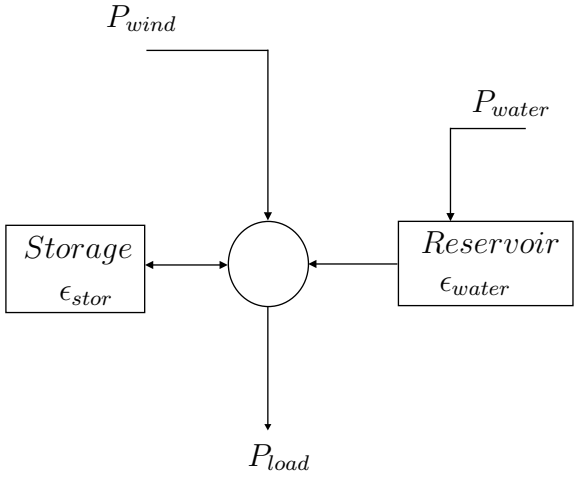

Figure 4.32: Model of power flow in a small power system with use of wind and hydro power system with storage capacity.

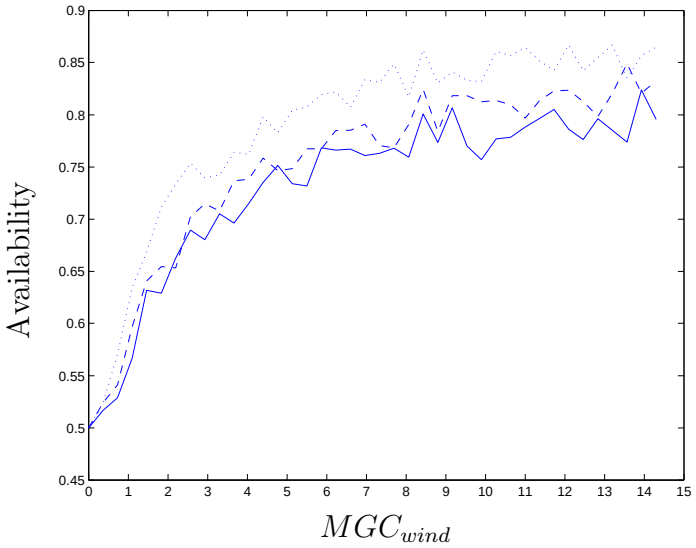

Figure 4.33: The availability of a power systems with wind and hydro power sources in combination with storage for different storage capacities. The solid line shows the availability for system with no storage while the dashed and dotted lines represent a storage capacity corresponding to one and three hours of maximum load, respectively.

In Figure 4.33 the flow-of-river is constant at 10% of maximum load and the reservoir capacity corresponds to one hour of maximum load.

In Table 4.2 the duration of shortages are shown for different levels of MGC_{wind}. The other parameters were constant and the same as for the case of solar and hydro power with storage. Increasing amount of wind capacity significantly reduces the number of long shortages (10 hours and longer). The total number of shortages also somewhat decreases.

Table 4.2: Number of shortages of different duration for different MGC_{wind}

Duration [h]	MGC_{wind}				
	1	2	5	10	20
1	16.0	31.7	39.7	39.5	42.8
2	11.4	25	35.1	31.9	37.1
3	10.4	21.2	26.2	28.8	27.8
4	9.4	18.7	23.2	21.5	22.8
5	8.8	19.1	19.1	21.4	18.6
6	9.8	15.7	18.8	16.7	14.9
7	10.3	16.6	16	13.6	15.2
8	13.8	14.8	15.3	12.5	12.8
9	21	15	14.5	11.9	11.0
10	42	29.9	16.2	13.4	14.3
11	121.2	87.2	63.1	51.9	37.8
12	117.6	69.5	32.7	16.9	7.1
Total shortages	391.9	364.5	319.8	280.1	263.4
Total hours	3746.3	2871.6	2103.0	1692.9	1425.8
Average h/short.	9.6	7.9	6.6	6.0	5.4

The main difference with the cases of solar-hydro-storage and solar-wind-storage are

for high values of MGC. In the solar-hydro-storage case the power source is more regular then in the solar-wind-storage case and that effects mainly the high MGC-values where the solar case has no shortages with a duration longer than 5.0 hours.

In Figure 4.34 the MGC_{wind} was 5.0 and the flow-of-river corresponded to 10% of the maximum load and the reservoir and storage capacity were corresponding to 1.0 hour of maximum load each. The main delivered power when the load is not supplied is between 10 and 20 % which is the contribution of the hydro power without wind and storage at daytime load.

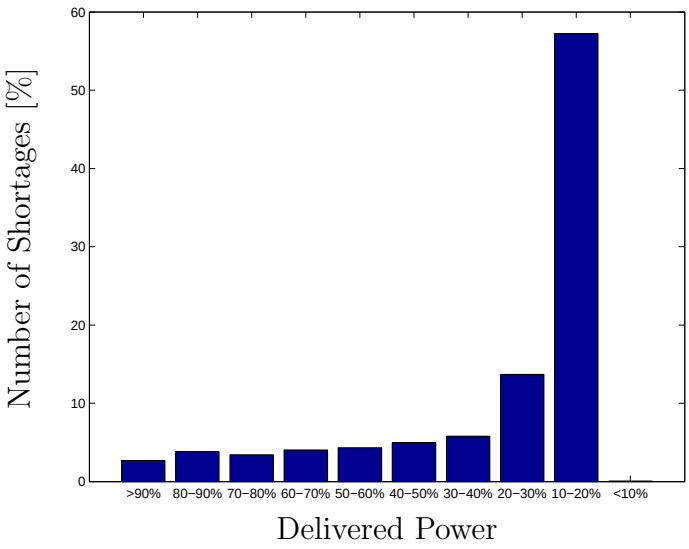

Figure 4.34: The generation capacity during the hours when the load was not fully supplied.

When the non-supplied hours occurs during the day. In Figure 4.35 the number of hours that is non-supplied shown for each hour of the day. The low number of shortages during night time is when the hydro power supplies the load completely. During daytime the hydro only supplies 10% of the load and then is the non-regular behavior of wind. During the morning hours the shortages are fewer than during the rest of the day because of the storage. In the figure $MGC_{wind} = 5$, storage capacity corresponds to one hour of maximum load and flow-of-river is 0.1 times the maximum load.

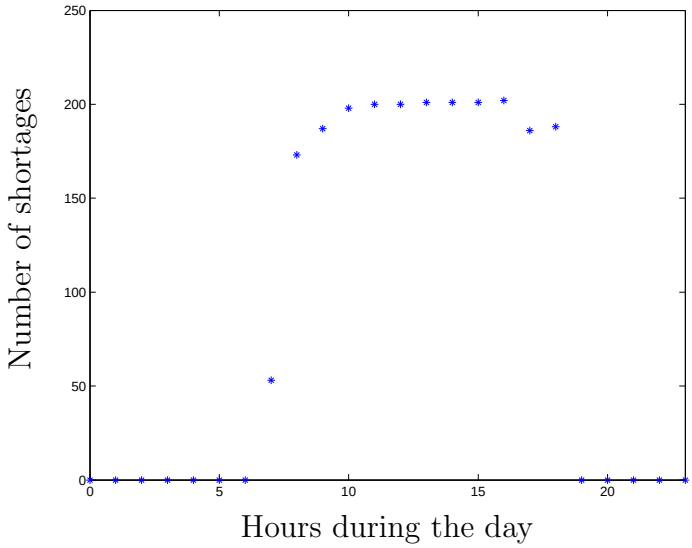

Figure 4.35: The hours of the day when the load was not fully supplied.

4.11 Solar, wind and hydro power

Another investigated case is a system, a model shown in Figure 4.36, with a combination of solar, wind and hydro power. The availability of such a system is shown in Figure 4.37, for different flow-of-river, and was calculated according to the equations below. The load was considered supplied if:

$$P_{sun} + P_{wind} + \epsilon_{water}(i) \geq P_{load} \tag{4.36}$$

The behavior of the water level in the reservoir was calculated from:

$$\Delta\epsilon_{water} = P_{load} - (P_{sun} + P_{wind}) \tag{4.37}$$

$$\epsilon_{water}(i+1) = \begin{cases} \epsilon_{water}(i) + P_{water} & \Delta\epsilon_{water} \leq 0 \\ \epsilon_{water}(i) + P_{water} - \Delta\epsilon_{water} & 0 < \Delta\epsilon_{water} < \epsilon_{water}(i) \\ P_{water} & \Delta\epsilon_{water} \geq \epsilon_{water}(i) \end{cases} \tag{4.38}$$

unless $\epsilon_{water}(i+1)$ exceeds ϵ_{water}^{max} because then should

$$\epsilon_{water}(i+1) = \epsilon_{water}^{max} \tag{4.39}$$

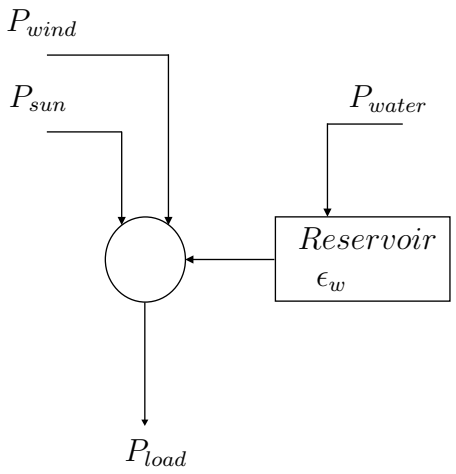

Figure 4.36: Model of power flow in a small power system with use of solar, wind and hydro power.

The Figure 4.37 the MGC_{wind} is constant and the MGC_{solar} varies. Here can also bee seen that the hydro limit of 0.1 time the maximum load (dotted and highest solid lines) is important to obtain high reliability.

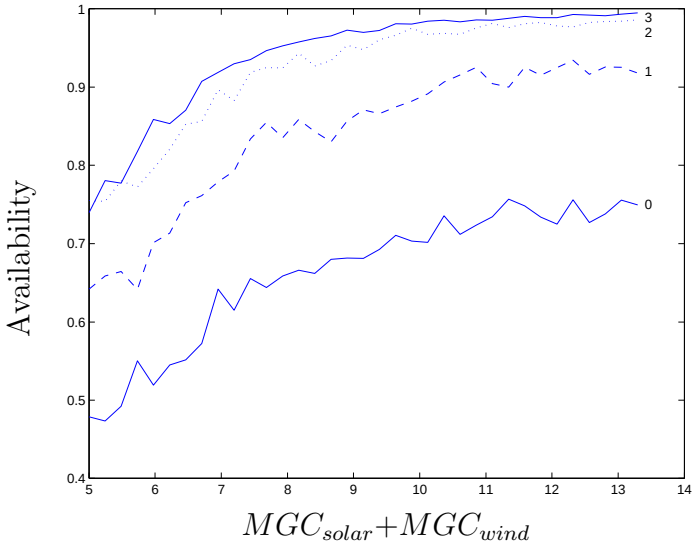

Figure 4.37: The availability of a power systems with solar, wind and hydro power sources for different flow-of-river. The solid line marked 0 the availability for system with no flow-of-river (no hydro) while the lines marked 1, 2 and 3 represents systems with flow-of-river that corresponds to 5%, 10% and 20% of maximum load, respectively.

Table 4.3 shows the duration of the shortages in the system with MGC_{wind} was set to 5.0 and the flow-of river corresponded to 10% of maximum load. The values of number of shortages in the table are the mean values of 25 independent simulations. The number of shortages decreases significantly with increasing MGC_{solar} because of the regularity of the solar power. The same behavior can be seen in Figure 4.1. The values are lower because of the power supplied from wind power.

Table 4.3: Number of shortages for different duration for different MGC

Duration [h]	MGC_{solar}				
	1	2	5	10	20
1	42.8	85.7	79.4	64.3	31.4
2	47.6	74.3	40.4	12.2	
3	46.4	43.2	20.6		
4	38.1	26.2	9.4		
5	24.9	14.9	3.3		
6	16.2	7.4	0.5		
7	9.6	5.4			
8	9.9	3.2			
9	7.3	2.7			
10	8	2.7			
11	38	14.6			
12	36.4	12.4			
Total shortages	325.2	292.7	153.6	76.4	31.4
Total hours	1798.2	877.5	279.1	88.7	31.4
Average h/short.	5.5	3.0	1.8	1.2	1.0

During the non-supplied hours there remains some available power for use, as can be seen in Figure 4.38. For the calculations of the delivered power, MGC_{solar} and MGC_{wind} were both set to 5.0, the flow-of-river was corresponding to 10% of maximum load,the reservoir capacity was corresponding to 1.0 hour of maximum load. A small amount of load shedding (20-30%) could significantly increase the availability.

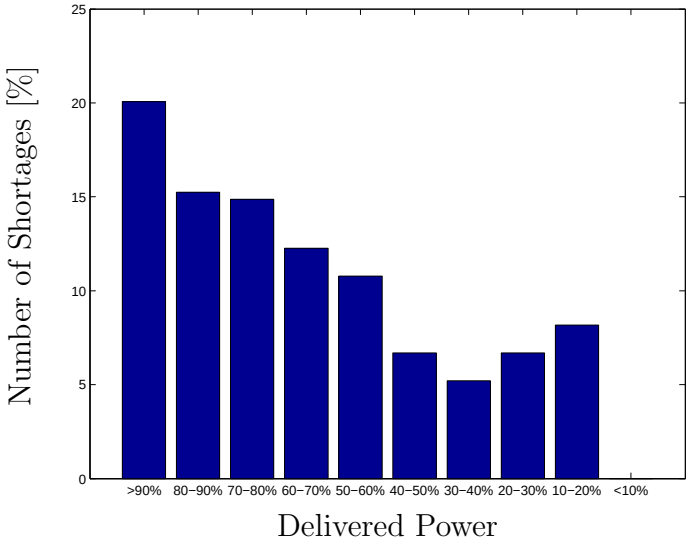

Figure 4.38: The available power during none fully supplied hours.

The shortages occur in the morning and in the evening, see Figure 4.39. The problem was earlier mentioned and the solution is adding some kind of storage to the system.

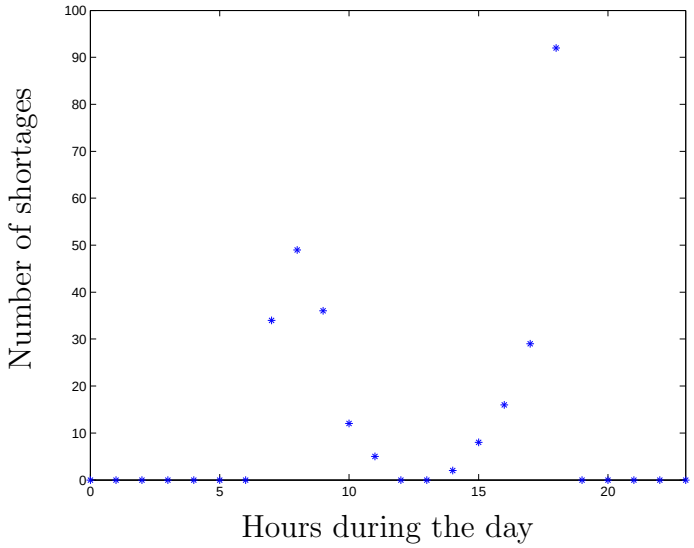

Figure 4.39: The hours during the day when shortages occurred.

4.12 Solar, wind and hydro power with ideal storage

A mentioned in the previous section the solar, wind and hydro power system gives a high availability but has some problem of supplying the load during morning and evenings. By adding storage a part of this problem could be solved. A model of a system with storage can be seen in Figure 4.40 and the availability for the system is shown in Figure 4.41. The load was considered supplied if:

$$P_{sun} + P_{wind} + \epsilon_{stor}(i) + \epsilon_{water}(i) \geq P_{load} \tag{4.40}$$

and the behavior of the storage and reservoir were:

$$\Delta\epsilon_{stor} = P_{load} - (P_{wind} + P_{sun}) \tag{4.41}$$

$$\Delta\epsilon_{water} = P_{load} - (P_{wind} + P_{sun} + \epsilon stor(i)) \tag{4.42}$$

$$\epsilon_{stor}(i+1) = \begin{cases} \epsilon_{stor}(i) - \Delta\epsilon_{stor} & \Delta\epsilon_{stor} < \epsilon_{stor}(i) \\ 0 & \Delta\epsilon_{stor} \geq \epsilon_{stor}(i) \end{cases} \tag{4.43}$$

$$\epsilon_{water}(i+1) = \begin{cases} \epsilon_{water}(i) + P_{water} & \Delta\epsilon_{water} \leq 0 \\ \epsilon_{water}(i) + P_{water} - \Delta\epsilon_{water} & 0 < \Delta\epsilon_{water} < \epsilon_{water}(i) \\ P_{water} & \Delta\epsilon_{water} \geq \epsilon_{water}(i) \end{cases} \tag{4.44}$$

if ϵ_{stor} and ϵ_{water} exceeds ϵ_{stor}^{max} and ϵ_{water}^{max}, respectively then

$$\epsilon_{stor}(i+1) = \epsilon_{stor}^{max} \quad \text{and} \quad \epsilon_{water}(i+1) = \epsilon_{water}^{max} \tag{4.45}$$

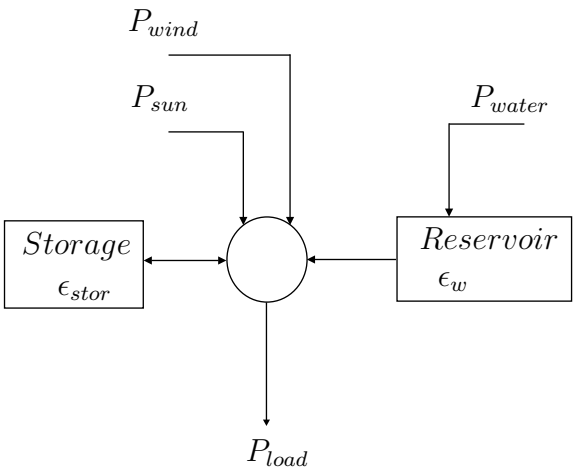

Figure 4.40: Model of power flow in a small power system with use of different renewable energy sources.

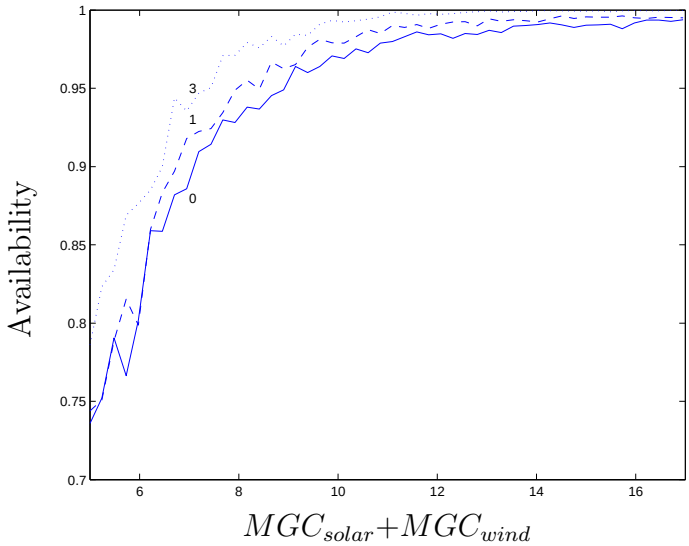

Figure 4.41: The availability for a system with solar, wind, hydro and different capacities of the storage. The numbers represents the capacities of the storage, corresponding to maximum load. MGC_{wind} was 5.0 for the calculation.

Durations of the shortages are shown in Table 4.4 and the differences between the number of shortages are increasing compared to the previous case 4.3 with increasing generation. That is because of the greater importance of the storage since more energy is produced and thereby is availably for storage and thereby later use. The values of number of shortages in the table are the mean values of 25 independent simulations.

Table 4.4: Number of shortages for different duration for different MGC

Duration [h]	MGC_{solar}				
	1	2	5	10	20
1	57.1	78.5	51.7	30.5	10.7
2	51.8	53.4	29.0	6.2	
3	45.0	34.2	14.9		
4	36.1	18.8	6.2		
5	23.6	11.0	1.4		
6	15.4	7.5			
7	8.2	4.6			
8	7.1	2.6			
9	6.6	2.4			
10	8.0	3.1			
11	33.3	11.3			
12	18.7	6.8			
Total shortage	310.9	234.2	103.2	36.7	10.7
Total hours	1494.8	774.6	186.2	42.9	10.7
Average h/short.	4.8	3.3	1.8	1.2	1.0

Power available during none-fully supplied hours of system with solar, wind and hydro power with storage are shown in Figure 4.42. The MGC_{solar} and MGC_{wind} were set to 5.0 and the flow-of-river corresponds to 10% of maximum load. The storage and the reservoir capacities corresponded to 1.0 hour of maximum load.

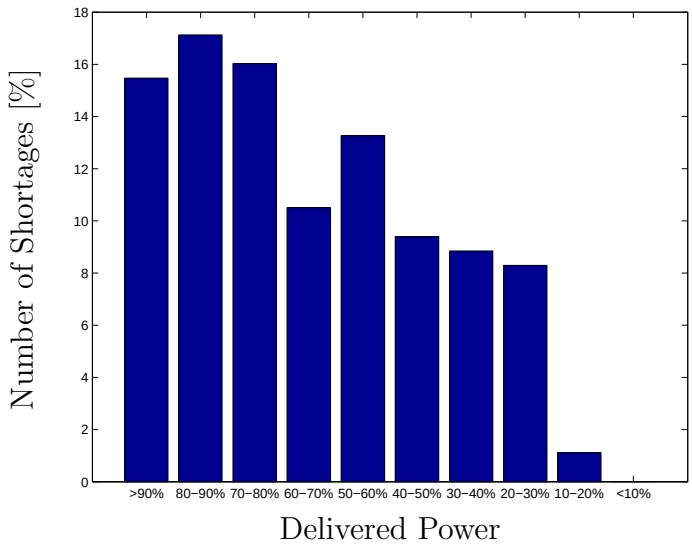

Figure 4.42: The available power for non-fully supplied hours.

In Figure 4.43 the times during the day when the shortages occur is shown. The behavior of the number of shortages is similar to the one in the case of solar, wind and hydro power without storage, see Figure 4.39, but the absolute numbers are lower. In this case can be seen that a load shedding of 30% will half the unavailability.

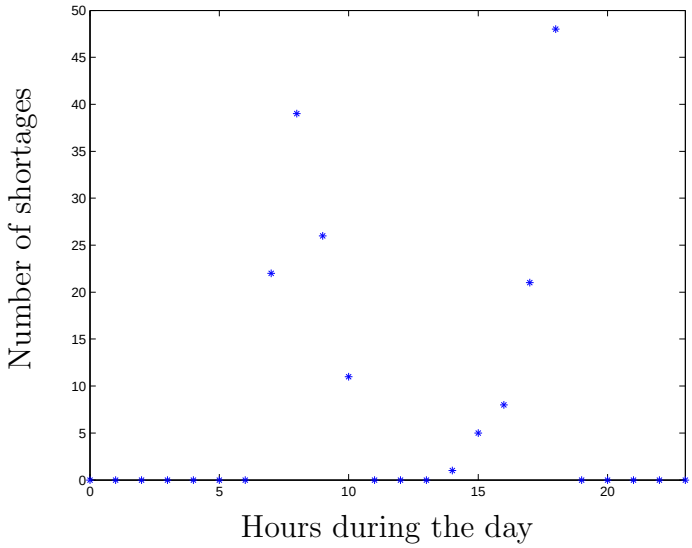

Figure 4.43: The available power for none-fully supplied hours.

4.13 Discussions of Case studies

One of the greatest differences between solar and wind power are the regularity of the solar power. This is both the advantage and the disadvantage of the solar power. Which one to use is dependent on the surrounding source, equipment and demand of course.

In the case of only one power source and no storage the one most available source is wind but the picture is a little more complicated. The overall availability is better for the wind power but that is only when the average is taken for the whole year. The solar power system has a significantly higher availability during daytime, see Table 4.5. Since the wind power only has a small difference between day and night time the large difference in the availability are due to the great difference in load between day and night time.

Table 4.5: Availability for night and day for solar and wind power

	Night	day
Solar power	0	0.61
Wind power	0.64	0.41

The same thing can be seen in Figure 4.44 where the high availability for solar during day time is shown by low number of shortages during daytime. For night time almost all the 4380 hours are not supplied. The wind power system has a more even distribution during the 24 hours period. The differences between day and night are due to earlier mentioned differences in the load.

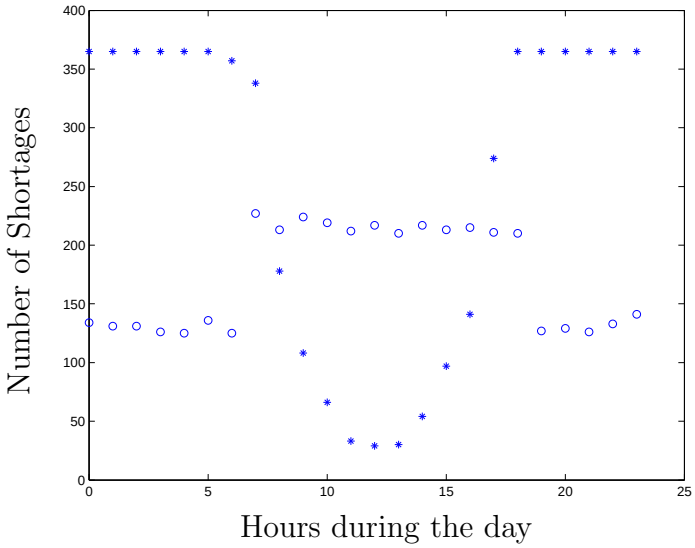

Figure 4.44: The hours during the day where solar and wind power system do not fully supplies the load. The asterisk represents the solar power system while the rings represents the wind power system.

With only one power source and no storage the availability will not exceed 0.7 (wind power) with reasonable installed power rate. If that has to be exceeded something else is needed to be added, storage, hydro power or combinations with solar and wind power.

Adding storage to a system will enhance the availability significantly, see Figures 4.9 and 4.22. The great difference in the two figures are due to the regularity of the solar power, which uses the storage capacity in a more effective way. The daily regular behavior of energy in the storage, as seen for solar power systems in Figure 4.10, is not noticeable for the wind power case, see Figure 4.23 and that is why the solar power system uses the storage in a more efficient way.

Adding hydro power and using the constant flow-of-river in combination a small reservoir is also something useful. The influence of flow-of-river is small except when the flow-of-river exceeds 10% of the maximum load, see Figures 4.12 and 4.31. The 10% of the maximum load is the load during the low load hours (night time) and that is why the solar and hydro power system has higher availability then the wind and hydro power system. If a power system has an availability of 100% of maximum load there are no need of some other power source.

By adding both the hydro power and storage possibilities the benefits from both could be used. The hydro for the night time and the storage for evening out the generation during day time. A solar power system gives also with this combination, a higher availability than a wind power based system due to more efficient use of the storage and hydro. The important factor is the regularity of the solar power and it can be seen in Tables 4.1 and 4.2. In the tables it can be seen that for MGC_{solar} above 5.0 there are no shortages with a longer duration then five hours while for the wind power based system shortages with duration of 12 hours occur even with a MGC_{wind} of 20.

Combining solar and wind power is not as effective as combining solar and hydro power.

But combining solar and wind power with storage possibilities have a higher availabil-

ity the solar and hydro power and the same as the solar and hydro power with storage. As can be seen in Figures 4.17 and 4.29 the case of solar and wind power based system has a more even distribution of the shortages during the day than the solar and hydro based system. A more even distribution is to prefer because the consequences of a shortage during day time (high load) will be worse then during night time (low load).

Combining solar, wind and hydro power and storage will be as expected even more beneficial for the availability. The shortages will occur during morning and evenings due to the lack of solar radiation.

In this discussion so far only fully supplied hours have been discussed. During a shortage the available power is not zero and the power could be used if the load is adapted to the situation. The available power during none-fully supplied hours is shown in this chapter for selected cases.

In this chapter the cases has all been discussed in an availability point of view but in almost every case the economical aspect is at least as important. But that aspect is not covered in this thesis.

Chapter 5

Conclusions

Two stochastic models are proposed in this thesis. A solar model based on cloud coverage is one of the models. A way to simulate cloud coverage data with reduced need for meteorological data is also presented. The second model is for simulating wind speed. It also reduces the need for meteorological measurements. Both the models are based on Markov theory.

A system with only one power source, only wind power has a higher availability than solar power but solar power has a more regular behavior. All power produced by solar is produced during daytime which will give higher availability during day-time than wind power.

Combining a single power source (wind or solar) with storage, the availability increases significantly. Solar power gives a higher availability because the regularity and thereby the more efficient use of the storage.

Adding a small hydro source in combination with wind or solar power will increase the availability further because it will supply the load during low load hours.

Combining solar and wind power gives a high reliability during daytime when both solar and wind power are available. The problem is during night-time when only wind is available. Adding hydropower covers the lowload period that occurs during night-time. The main problems occur when the high day-time load begins before the solar power is available at sufficient extent and at dusk when the load is still at day-time level.

To be able to use exclusively renewable energy sources a combination of sources is needed to secure the reliability of the supply. It is also important to adjust the load levels to the availability of the renewable sources.

Chapter 6

Future Work

This thesis is just a small part of the research area addressed. The area of isolated power systems based entirely on renewable energy is just in its cradle. There are many aspects that are not investigated in this thesis and that is something for future work.

Probably most important are the economical aspects for this kind of systems. It is important to keep the focus on supplying activities that could generate income to the area, like products that can be sold outside of the area.

In the case studies and in the models all components have been assumed ideal and the non-ideal behavior is something to include. This would require more detailed knowledge of the components used.

One of the larger problems of introducing new technologies is the social acceptance, especially when the level of technology is low before the introduction. The reliability and robustness of the system required for social acceptance also need to be further investigated.

The models presented in this thesis are independent. Future development of the models would be to introduce dependencies between wind, sun and the supply of hydro power. That dependencies exists is obvious for a extreme dry year the supply of hydro will be bad but the solar power will then be larger. More generally, each of these sources will show a seasonal variation.

In this thesis the load model is deterministic and that is just a rough estimation of the a real load. The load model should also be stochastic and even dependent on meteorological conditions. The stochastic element becomes more important in a small system. Some loads are weather-dependent which introduces additional dependencies. Further investigations should include load-shedding policies when low generation capacity is expected.

The power system use in this thesis has been modelled as a single node. By introducing a realistic power system some other aspects would need to be studied like thermal overload during warm weather.

How should this systems be controlled? What kind of power electronics equipment is

needed? That are other important questions that have to be answered before use of isolated power systems with only renewable energy sources.

References

[1] R. Billinton and R. Allan, *Reliability Evaluation of Power Systems*. Plenum Press, 1996.

[2] B. Lindgren, *Power-generation, Power-electronics and Power-systems issues of power Converters for photovoltaic applications*. Chalmers University of Technology, 2002.

[3] L. Johnson, *Wind Energy Systems*. Prentice-Hall, Inc., 1985.

[4] P. Sørensen, A. Hansen, and P. Rosas, "Wind models for simulation of power fluctuations from wind farms," *Journal of Wind Engineering and Industrial Engineering*, vol. 90, no. 12, pp. 1381–1402, 2002.

[5] A. Høyland and M. Rausand, *System Reliability Theory - Models and Statistical Methods*. John Wiley & Sons, Inc., 1994.

[6] R. Gallager, *Discrete Stochastic Processes*. Kluwer Academic Publishers, 1996.

[7] S. Ross, *Introduction to Probability Models*. Academic Press, Inc., 1989.

[8] R. Billinton and W. Li, *Reliability Assessment of Electric Power Systems Using Monte Carlo Methods*. Plenum Press, 1994.

[9] G. Fishman, *Monte Carlo - Concepts, Algorithms and Applications*. Springer, 1996.

[10] U. Amato, A. Andretta, B. Bartoli, B. Coluzzi, V. Cuomo, F. Fontana, and C. Serio, "Markov processes and fourier analysis as a tool to describe and simulate daily solar irradiance," *Solar energy*, vol. 37, no. 3, pp. 179–194, 1986.

[11] D. Albizzatia, G. Rossetti, and O. Alfano, "Measurements and predictions of solar radiation incident on horizontal surfaces at Santa Fe, Argentina (31° 39'S, 60° 43'W)," *Renewable Energy*, vol. 11, no. 4, pp. 469–478, 1997.

[12] A. Balouktsis and P. Tsalides, "On stochastic simulation of hourly total solar radiation sequences," *International Journal of Energy Systems*, vol. 8, no. 3, pp. 1121–125, 1988.

[13] V. Graham and K. Hollands, "A method to generate synthetic hourly solar radiaition globally," *International Journal of Solar Energy*, vol. 44, no. 6, p. 333, 1990.

[14] A. Balouktsis and P. Tsalides, "Stochastic simulation model of hourly total solar radiation," *International Journal of Solar Energy*, vol. 37, no. 2, p. 119, 1986.

[15] R. Stull, *Meteorology Today For Scientists and Engineers: A Technical Companion Book*. West Publishing Company, 1995.

[16] L. Nielsen, L. Prahm, R. Berkowicz, and K. Conradsen, "Net incoming radiation estimated from hourly global radiation and/or cloud observations," *Journal of Climatology*, vol. 1, no. 3, p. 255, 1981.

[17] P. Jones, "Cloud-cover distribution and coorrelations," *Journal of Applied meteorolgy*, vol. 31, p. 732, 1992.

[18] U. Hjort, *Computer Intensive Statistical Methods: Validation, Model Selection and Bootstrap*. Chapman & Hall, 1995.

[19] G. Boyle, *Renewable Energy - power for a sustainable future*. Oxford University Press, 1996.

[20] M. Svensson, F. Zhang, S. Veenstra, W. Verhees, J. Hummelen, J. Kroon, O. Inganäs, and M. Andersson, "High-performance polymer solar cells of an alternating polyfluorene copolymer and a fullerene derivative," *Advanced Materials*, vol. 15, no. 12, pp. 988–991, 2003.

[21] M. Green, K. Emery, D. King, S. Igari, and W. Warta, "Solar cells efficiency tables (version 22)," *Progress in Photovoltics: Reasearch and Applications*, vol. 11, no. 5, pp. 347–352, 2003.

[22] http://www.nwp.se, "Tekniska data: Nordic 1000."

[23] R. Billinton and L. Gan, "Wind power modeling and application in generating adequacy assessment," in *IEEE WESCANEX 93. Communications, Computers and Power in the Modern Environment Conference Proceedings*, (Saskatoon, Sask., Canada), pp. 100–106, May 17-18, 1993.

[24] S. Biswas, B. Sraedhar, and Y. Singh, "A simplified statistical technique for wind turbine energy output estimation.," *Wind Engineering*, vol. 19, no. 3, pp. 147–155, 1995.

[25] A. Feijoo, J. Cidras, and J. Dornelas, "Wind speed simulation in wind farms for steady-state security assessment of electrical power systems," *IEEE transactions on Energy Conversion*, vol. 14, no. 4, pp. 1582–1588, 1999.

[26] L. Kamal and Y. Jafri, "Time series models to simulate and forecast hourly averaged wind speed in Quetta, Pakistan.," *Solar Energy*, vol. 61, no. 1, pp. 23–32, 1997.

[27] P. Sparis, J. Antonogiannakis, and D. Papadopoulos, "Markov matrix coupled approach to wind speed and direction simulation," *Wind Engineering*, vol. 19, no. 3, pp. 121–133, 1999.

[28] C. Masters, J. Mutale, G. Strbac, S. Curcic, and N. Jenkins, "Statistical evaluation of voltages in distribution systems with embedded wind generation.," *IEE Proceedings-Generation, Transmission and Distribution*, vol. 147, no. 4, pp. 217–212, 2000.

[29] G. Ronsten, S.-E. Thor, H. Ganander, H. Johansson, T. Thiringer, T. Petru, and H. Bergström, "Evaluation of loads, power quality, grid interaction, meteorological condition and power performance of this first swedish offshore wind farm at Bockstigen," in *(OWEMES ´00)*, (Syracuse, Italy), April 13-14, 2000.

[30] *Gold Book; Recommended Practice for the Design of Reliable Industrial and Commercial Power Systems*. IEEE Inc., 1998.

[31] G. Notton, M. Muselli, P. Poggi, and A. Louche, "Decentralized wind energy systems providing small electric loads in remote areas.," *International journal of energy research*, vol. 25, pp. 141–164, 2001.

[32] T. Ackermann and L. Söder, "An overview of wind energy-status 2002," *Renewable and Sustainable Energy Reviews*, vol. 6, no. 1-2, pp. 67–128, 2002.

[33] A. Price and B. Davidson, "Recent developments in the design and applications of utility-scale energy storage plant," in *Electricity Distribution, 2001. Part 1: Contributions. CIRED. 16th International Conference and Exhibition on*, (Amsterdam, Netherlands), p. 4.22, 18-21 June, 2001.

[34] J. McDowall, "Nickel-cadmium batteries for energy storage applications," in *Battery Conference on Applications and Advances, 1999. The Fourteenth Annual*, (Long Beach,CA,USA), pp. 303–308, 1999.

[35] S. Schoenung and C. Burns, "Utility energy storage applications studies," *IEEE transactions on Energy Conversion*, vol. 11, no. 3, pp. 658–665, 1996.

[36] P. Ribeiro, B. Johnson, M. Crow, A. Arsoy, and Y. Liu, "Energy storage systems for advanced power applications," *Proceedings of the IEEE*, vol. 89, no. 12, pp. 1744–1756, 2001.

[37] T. Sels, C. Dragu, T. Van Craenenbroeck, and R. Belmans, "Overview of new energy storage systems for an improved power quality and load managing of distribution level.," in *Electricity Distribution, 2001. Part 1: Contributions. CIRED. 16th International Conference and Exhibition on*, (Amsterdam, Netherlands), p. 4.26, 18-21 June, 2001.

[38] M. Bollen, *Understanding power quality problems: voltage sags and interruptions*. IEEE Press, 2000.

[39] J. Boyes and N. Clark, "Technologies for energy storage. flywheels and super conducting magnetic energy storage.," in *Power Engineering Society Summer Meeting, 2000. IEEE*, (Seattle, WA, USA), pp. 1548–1550, 2000.

[40] L. Reinke and P. Eng, "Tutorial overview of flywheel energy storage in a photovoltaic power generation system," in *Electrical and Computer Engineering, 1993. Canadian Conference on*, (Vancouver, BC, Canada), pp. 1161–1164, 1993.

[41] I. Grant, "Tva's regenesys energy storage project," in *Power Engineering Society Summer Meeting, 2002 IEEE*, (Tennessee Valley Authority, Chattanooga, TN, USA), pp. 321–322, 2002.

[42] V. Karasik, K. Dixson, B. Weber, G. Campbell, and P. Ribeiro, "SMES for power utility applications: A review of technical and cost considerations," *IEEE transactions on applied superconductivity*, vol. 9, no. 2, pp. 541–546, 1999.

[43] C. Loungo, "Superconducting storage systems: An overview," *IEEE Transactions on Magnetics*, vol. 32, no. 4, pp. 2214–2223, 1996.